Material Science, Department of

Theses-Material Science

African University of Science and Technology Year 2010

Gold Nanoparticles for Medicine

Richard Botah

African University of Science and Technology-Abuja, Dept. of Material Science,
richbotah@yahoo.co.uk

GOLD NANOPARTICLE FOR MEDICINE

THESIS

Presented to the Graduate Council of
African University of Science and Technology-Abuja
in Partial Fulfillment
of the Requirements

for the Degree
Master of SCIENCE

By
Richard Botah

FCT, Abuja

December 2010

GOLD NANOPARTICLES FOR MEDICINE

Committee Members Approved:

_____

Winston W. Soboyejo

_____

Kwadwo Osseo-Asare

_____

Douglas Buttrey

Approved by:

_____

COPYRIGHT

by

Richard Botah

DEDICATION

For: My Mom, Alice.

ACKNOWLEDGEMENT

I would like to express my deepest gratitude to my wonderful mom, Alice. Throughout the course of my graduate studies, she has been extremely supportive. Without her love and support, I never could have made it this far. I would also like to thank my wonderful friend, Ivy, who inspires me to strive for success and who motivates me to attain my full potential. Furthermore I would like to thank the Botah family and my uncle, Eric and, for their support throughout my life and my education.

Academically and professionally I owe a great debt of gratitude to Prof Soboyejo, who took on the arduous task of becoming my research advisor. I am also thankful to Dr.Shola Odusanya who supervised my work throughout my stay in the Biotechnology laboratory in SHESTCO. The knowledge I have gained from them is invaluable, and I feel privileged to have had the opportunity to work under their supervision. I also want to thank Prof Douglas Buttrey and Prof Kwadwo Osseo-Asare for serving on my committee; I owe additional thanks to Esther Yeboah for her immense contribution to my studies. Finally I would like to thank Joseph Asare, Joseph Akurang, Azubuike Michael and all my course mates; Auphedeous, Omena, Damilola and Mustapha for all their assistance throughout this study and my stay at African University of Science and Technology.

This manuscript was submitted on December, 2010.

TABLE OF CONTENT

LIST OF TABLES

LIST OF FIGURES

ABSTRACT

Gold nanoparticles were synthesized by reducing aqueous chloroauric acid ($HAuCl_4$) with three different bacteria. Various microorganisms were verified to see how feasible they will be in synthesizing gold nanoparticles. Three microorganisms were screened and found to produce gold nanoparticles effectively. These bacteria include; Bacillus megaterium, Bacillus subtilis and serratia mercensis mercensis. Microorganisms in the synthesis of nanoparticles appear as an environmentally friendly and exciting approach. Different sizes and shapes of gold nanoparticles are produced by the various microorganisms used. The particle sizes and shapes were controlled by pH. The microorganisms and the $HAuCl_4$ were incubated at pH of 3 and 7. It was observed that spherical nanoparticles were observed at of pH 7 whiles nanoplates were observed at pH 3.

Poor bioavailability and intrinsic toxicity are some of the problems facing conventional therapies and as a result have compromised the therapeutic efficacy of many otherwise beneficial drugs. Some of these shortcomings of the conventional therapies are been overcome by the design of nanoscopic systems to change the pharmological and therapeutic properties of molecules. In order to enhance the bioavailability of targeted site, nanosystems are often accumulated at higher concentrations than normal drugs. Systems toxicity is greatly reduced when the enhanced drug is targeted to the diseased tissue.

Diagnosis of cancer is often late as most of them are hidden or known metastasis. The ability of gold nanoparticles to absorb light in the visible and near-infra red (NIR) region depends strongly on the shape and size of the nanostructure. Moreover, the amount of cells that can be taken by gold nanoparticles is size dependent with optimal diameter of 50 nm for spherical nanoparticles.

CHAPTER ONE

1.0 INTRODUCTION

1.1 Statement of Introduction and Background

Synthesis of metal nano particles has received much attention in recent times because of their numerous applications in catalysis [3], sensor technology [1], biological labeling [5], optoelectronics recording media and optics [2]. The mode of producing these nano particles can be done by chemical, biological and physical methods [3, 6]. Chemical and physical methods were mostly used in synthesizing gold nanoparticles; however there has been an appreciable rise in the biological synthesis of nano particles in the past decade. This is because biological synthesis is ecologically friendly. Moreover, the method is non toxic and produces a clean product.

Nanoparticles are particles with one or more dimensions on the order of nano particles (10^{-9} meters) [7]. Nano scale region has received much attention in material science in recent years because of their numerous potential applications. There has been significant research work to describe particles of this size. Since particles of nano meter behave differently from their bulk size counterparts, research work to describe particle size has been challenging. This is seen when the physical properties of the material changes when the particle size decreases. This phenomenon comes about when physical quantities, such as magnetic domain size, grain size etc have similar size.

Nano scale research is of significant contribution in material science and technology for the development of new materials with improved properties. Wear resistance, elasticity, strength, thermal conductivity, electrical conductivity etc are some of the properties of importance. Materials to perform effective, efficient and complex tasks have also been researched. The medical application of nano technology and related research is nano medicine. Nano medicine comprises of the various medical applications of nano materials to medicine.

In medical application system, nano particles are been used to deliver drugs, heat, light or other substances to cells such as cancer cells. Direct treatments of diseased cells are made possible when engineered particles are attracted to the diseased cells. X ray activated nanoparticles have the capacity to destroy cancer cell which cling to them. The damage caused to healthy tissue by this method is much less than in radiation therapy. Moreover nano particles such as alumno-silicates reduce bleeding quickly in traumatic patients by clotting blood quickly and absorbing water. In diagnostic and imaging techniques cancer tumors in patients can be located using quantum dots (qdots). Magnetic Resonance Imaging (MRI) images of cancer tumors also can be improved using iron oxide nanoparticles. Disease indicators can be detected at the early stages when nanoparticles are allowed to attach themselves to protein or other molecules.

Like most metals, gold nanoparticles can be produced. As a pure and a naturally occurring element, gold is very unreactive, malleable and ductile. However it reacts in a mixture of acids such as aqua regia and cyanide solutions. Gold has the ability to dissolve in mercury but it does not react with it and does not oxidize in water. Gold normally occurs in alluvial deposits, nuggets or occurs in veins.

Gold has been used as a monetary value since history because it is a precious metal. Furthermore, it is also used in jewelry such as chains, bracelets etc. Apart from its traditional uses, gold is also used in many industrial applications. Due to its resistance to oxidative corrosion and as a good conductor of electricity, gold is used in dentistry and electronics. It is also used in the food and drink industry.

The non reactivity property of gold facilitates its use in medicine. In diagnosis, radioactive gold is monitored as a beta emitter, as it passes through the body when it is injected in a colloidal solution. For a person who finds it difficult to close the eyes completely, i.e. lagophthalmos, gold particles are used to remedy the condition by impacting the gold nano particles in the upper eyelid. Moreover certain cancers are treated by implanting radioactive gold isotope in tissues to serve as radioactive sources. Gold also finds application in dentistry as a result of its aesthetic appeal and also for filling cavities.

1.2 Problem Description and Scope of Work

The purpose of this project is to study gold nanoparticles within the context of potential applications in nano-medicine. The adhesion of gold is studied within the context of nanoparticle clusters with the potential for use in cancer detection and treatment. The potential for hyperthermic treatment is also explored along with the biosynthesis of gold nanoparticles. Following the introduction, prior work on gold nanoparticles is reviewed in chapter 2. Their potential applications in medicine and its potential heating via hyperthermia are explored in chapter 3. The biosynthesis of gold, adhesion of gold nanoparticles and other experimental procedures are presented in chapter 4. The final chapter gives results, conclusions and suggestions for future work.

1.3 References.

[1] Gomez-Romero P (2001) Hybrid organic-inorganic materials—in search of synergic activity. Adv Mater 13:163– 174

[2] Gracias DH, Tien J, Breen T, Hsu C, Whitesides GM (2002) Forming electrical networks in three dimensions by self-assembly. Science 289:1170–1172

[3] Lim JK, Kim Y, Lee SY, Joo SW (2008) Spectroscopic analysis of L-histidine adsorbed on gold and silver nanoparticle surfaces investigated by surface-enhanced Raman scattering. Spectrochim Acta A 69:286–289

[4] Narayanan R, EI-Sayed MA (2004) Shape-dependent catalytic activity of platinum nanoparticles in colloidal solution. Nano Lett 4:1343–1348

[5] Qiu H, Rieger B, Gilbert R, Jerome C (2004) PLA-coated gold nanoparticles for the labeling of PLA biocarriers. Chem Mater 16:850–856

[6] Shiv Shankar S, Rai A, Ankamwar B, Singh A, Ahmad A, Sastry M (2004a) Biological synthesis of triangular gold nanoprisms. Nat Mater 3:482–488

[7] Online. www.malvern.com/labeng/industry/nanotechnology/nanoparticles_definition.htm

CHAPTER TWO

2.0 LITERATURE REVIEW

2.1 Introduction

Gold nanoparticles preparation is increasingly becoming an important research area which requires all aspects of science in recent times. As a result of its properties, gold nanoparticles have lots of applications. This could be seen in field of catalysis [11, 14], electronic and electro-optical devices [15, 17], biomedicine [18-22], imaging, etc. Size and shape are very important in the physiochemical and optoelectronic properties of nano materials [4, 6]. As a result of this, the applications of gold nanoparticles are due to the different shapes and sizes that are found when synthesized.

Until recently, most of the methods used in producing gold nanoparticles were chemically based. [7, 10]. It is in this light, that alternative methods of producing gold nanoparticles are been explored. The aim is to be able to produce particles which are clean, non toxic and technologies without negative effect on the environment. Some bacteria and fungi have been able to synthesize gold nanoparticles. This has been possible because microorganisms have the ability to resist heavy metal ions in bioprocessing of metal by reduction or metal sulfides formation [10].

This chapter reviews prior works on the processing and properties of gold nanoparticles for potential applications in medicine. The potential applications of gold nanoparticles in hyperthermia and drug delivery are also explored. Other works of producing gold nanoparticles chemically, with different microorganisms and plant extract will also be reviewed.

2.2 Electrochemistry

Electrochemistry is an aspect of chemistry that involves chemical reactions in solutions which consists of a conductor (metal or semiconductor) and ionic conductor (electrolyte). There exist

the transfer of electrons in solution between the electrode and the electrolyte. An electrochemical reaction occurs when the chemical reaction proceeds either by an external applied voltage (electrolysis) or when the voltage is obtained from the chemical reaction occurs when electron transfer are between [33].

2.2.1 Redox Reaction

Redox is reduction-oxidation. It involves electron transfer between molecules or ions. Oxidation states of these molecules and ions change in the process. The reaction can proceed by applying external voltage or through the release of chemical energy [33].

Oxidation and reduction involves change in the oxidation state of molecules, atoms or ions involved in the electrochemical reaction. There is an increase in the oxidation state when an atom or ion gives up an electron; however the oxidation state of the receiver decreases. Oxidation and reduction proceeds in a way such that one of the species is oxidized the other is reduced. Redox reaction thus occurs as a result of the paired electron transfer.

A reaction between sodium and chlorine proceeds in a way that, sodium donates one electron to the chlorine. In the process, sodium attains oxidation state of +1 whereas chlorine acquires -1.

Oxidation occurs when an atom loses an electron whiles reduction is the gain of electron by an atom. A reducing agent is the atom or molecule which loses electrons. Oxidizing agents or oxidants accept electron. A common oxidizing agent is oxygen. Fluorine is known to be a stronger oxidant than oxygen. An atom is oxidized when oxygen is added. Oxygen is reduced in the process. For organic compounds, a molecule is oxidized when there is loss of hydrogen. This is due to the fact that hydrogen donates its electron in covalent bonds with non metals.[33]

Balancing of Redox reactions

Balancing redox reaction brings the understanding in electrochemical reactions in water. The Ion electron method is used, whereby H^+, OH^- H_2O and electrons are added to cells half reaction for oxidation and reduction.

2.2.1.1 Acidic medium

Unbalanced reaction: Mn^{2+} (aq) + $NaBiO_3$(s) → Bi^{3+} (aq) + MnO_{4-} (aq)

Oxidation: 4 H_2O (l) + Mn^{2+} (aq) → MnO_4^-(aq) + 8 H^+ (aq) + 5e^-

Reduction: 2 e^- + 6 H^+ (aq) + BiO_3^- (s) → Bi^{3+} (aq) + 3 H_2O (l)

Reaction balanced:

14 H^+ (aq) + 2 Mn^{2+} (aq) + 5 $NaBiO_3$ (s) → 7 H_2O (l) + 2 MnO_4^- (aq) + 5 Bi^{3+} (aq) + 5 Na^+ (aq) [33]

2.2.1.2 Basic medium

OH^- ions and water are used in balancing the overall reaction in basic medium. Considering a reaction between potassium permanganate and sodium sulfite.

Unbalanced reaction: $KMnO_4$ + Na_2SO_3 + H_2O → MnO_2 + Na_2SO_4 + KOH

Reduction: 3 e^- + 2 H_2O + MnO_4^- → MnO_2 + 4OH^-

Oxidation: 2 OH^- + SO_3^{2-} → SO_4^{2-} + H_2O +2e^-

Equation balanced:

2 $KMnO_4$ + 3 Na_2SO_3 + H_2O → 2 MnO_2 + 3 Na_2SO_4 + 2 KOH [33]

2.2.1.3 Neutral medium

The same procedure as used on acid medium is applied, for example on balancing using electron ion method to complete combustion of propane.

Unbalanced reaction: $C_3H_8 + O_2 \rightarrow CO_2 + H_2$

Reduction: $4\ H^+ + O_2 + 4\ e^- \rightarrow 2\ H_2O$

Oxidation: $6\ H_2O + C_3H_8 \rightarrow 3\ CO_2 + 20\ e– + 20H^+$

Equation balanced:

$C_3H_8 + 5\ O_2 \rightarrow 3\ CO_2 + 4\ H_2O$ [33]

2.3 Synthesis of Gold Nanoparticles Methods

Several approaches have been used for the synthesis of gold nanoparticles. Synthesizing of gold nanoparticles can be done either chemically, biologically or physically [36]. The eventual product should be clean, non toxic and should not have negative impact on the environment.

2.3.1 Biosynthesis processes

2.3.1.1 Phyllantin assisted biosynthesis of gold nanoparticles. A novel biological Approach.

This method of synthesizing gold nanoparticles was developed by Kasthuri et al.

The Phyllantin plant is dominant specie in South India. The plant has many uses in area of medicine. Some of these include uses as antiviral agents for the treatment of hepatitis B, gastropathy, diarrhea, dysentery, scabies, ulcers, asthma and wounds [1].

Separation of the Phyllantin from the phyllantin amarus plant

The process of separation of the Phyllantin and the hypophyllantin was achieved by mixing the leaf powder with the slaked lime prepared in petroleum ether in the proportion 10:3 to prevent the extraction of chlorophyll. It was observed that the shape change from hexagonal to spherical was immense when the concentration of the extract was changed.

Kasthuri et al revealed that Phyllantin, hypophyllantin, carotenoids and wax were the constituents of the extract. Methanol addition helped to remove wax from the extractors whiles phyllantin and hypophyllantin were obtained in almost pure conditions [34]. Crystallization was used to obtain a pure sample of hypophyllantin and phyllantin, from the petroleum ether or methanol. In all the fractional crystallization, hypophyllantin separated out first whiles the other components followed. UV-visible spectroscopy [λ max 278nm, 10.226; 210nm (2.360) and mass spectroscopy] was used to determine the purity of the phyllantin.

It was observed that, at different concentrations of phyllantin extract, the UV spectra were in the visible and near infra-red regimes, for the various concentrations varied after complete reduction of the chloroauric acid. The colour change observed was also the result of the surface plasmon resonance (SPR). When the concentrations of the extract were changed, two things were identified. The transverse plasmon resonance absorption peak was seen at 540nm. There was a minimum shift to shorter wavelength along with increasing the intensity. Moreover, the relative intensity and the position of the second band appeared in the NIR region of the electromagnetic spectrum along with the red shift known as the longitudinal plasmon resonance band. The formation of triangular and hexagonal shaped gold nanoparticles resulted in this band [3]. Low concentration of extract resulted in this.

2.3.1.2 Biosynthesis of gold nanoparticles using the bacteria Rhodopseudomonas Capsulata

A biological process for synthesizing gold nanoparticles has been developed was by He et al []. Some microorganisms that were found to pose no problems to the environment and the ecology have also been shown to synthesize gold nanoparticles. An example of such organism is prokaryote bacteria rhodopseudomonas capsulata. This organism is found in the natural environment, and has the potential to reduce Au^{3+} ions at room temperature using a one-step approach. Gold nanoparticles were produced at lower pH using this microorganism.

From the results, there was a reduction in the aqueous chloroaurate ions when they were exposed to the bacteria. This was seen in the colour change from pale yellow to purple. This proves the extracellular gold nanoparticles formation. Other experiments done with no biomass additions

revealed evidence of no colour change. It was also observed by that the reaction solution has an absorption maximum at about 540nm. A Surface plasmon resonance band was acknowledged to be the reason for this value.

2.3.1.3 Photochemical Synthesis of Gold nanoparticles by the sunlight radiation using a seeding approach

Dong et al [35] have proposed a method for synthesizing gold nanoparticles. This process considers gold nanoparticles of controlled sizes from a photochemical and seeding approach. The ability to use UV solar radiation and seeding approach simultaneously made it possible to harness solar energy for controlling the size of gold nanoparticles produced. Moreover particles, which are expected to be large, can be grown from smaller size without using seed-mediated nucleation processes. Functional nanoparticles are produced by poly ethylene glycol (PEG). This takes place ligand exchange reactions. Again chloride ions are removed in the photochemical reduction reaction when they were used as precursors of a preparing catalyst. Lastly, the method is simple, less costly and convenient.

An electronic dual light transilluminator (ultra lumcon) was used as a light source when the gold seed particles were prepared. At the first stage of nucleation, the stirring was done lightly. There was a colour change of the solution to ruby red. This was used as a seed solution.

A Seed-mediated growth approach under UV solar radiation was used in synthesizing larger gold particles. Three procedures were in a stepwise synthesis. In the first step, Au (III) ion was added to PEG (MW 600) and acetone aqueous solution. The gold seed concentration remained constant at 2.44×10^{-4} M/L, with a molar ratio of seed and ion been 1/11.5. There was a change in the surface plasmon absorption when the solution was left in the sun for 50 minutes. In the second step, the concentration of the seed particles and Au (III) ion was 1.22×10^{-3} M/L with a molar ratio of seed and ion been 1/57.5. Even though the gold particles produced in the first step was used as a generation seed for larger particles in the third procedure, the total concentration and the molar ratio of gold seed were similar to the first procedure.

The effect of acetone on the making of the good seed particles by the UV irradiation was studied Dong et al [35]. It was observed that the surface plasmon absorption band occurred at 520 nm, while the induction period for the production of the nanoparticles in the presence of acetone was quite short, about 15 mins.

At the initial stage of radiation exposure, atoms formed have shorter lifetime and are very reactive. Moreover, their surface can be used as an autocatalytic growth center which can promote the reduction of gold ions in solution. After 10 mins exposure to radiation, the colour of the solution changed to ruby red with a surface plasmon absorbance band of 516 nm. With increasing in irradiation time, the absorbance did not increase. This confirms the whole reduction was by photochemical reactions that produce gold nanoparticles. It also reveals that the nucleation and growth of gold nanoparticles occurred at a rapid rate. The Induction period was 12mins after 35 mins of irradiation, when acetone was not added. The plasmon absorption band maximum shifted to 524.5 nm after the reaction.

During TEM analyses, it was observed that spherical gold particles were formed when acetone was added. The average diameter of particles obtained was 5 nm with a narrow size distribution. In contrast, a broad size distribution of gold particles was obtained in the absence of acetone. Therefore for the size and shape controlled synthesis of increasing gold nanoparticles in the PEG and acetone aqueous solution system, 5 nm gold particles can be used as seeds.

The above results, therefore suggest that the seed-mediated growth of Au nanoparticles is strongly influenced by UV solar energy.

2.3.2 Chemical Synthesis Processes

Introduction

There are many advanced ways of producing gold nanoparticles. However, the most common way of producing gold nanoparticles is by the reduction of chloroauric ($HAuCl_4$) in a liquid. A reducing agent is added just after stirring to cause gold ions ($Au^{3+)}$ to reduce to gold atoms (Au). Supersaturation is attained when the gold atoms are formed continuously. The gold is then

precipitated in sub-nanometer particles. Stabilizing agents can be added to the surface of nanoparticles from forming aggregates. Organic-inorganic hybrids with improved applications can be produced with various organic ligands [23].

2.3.2.1 Turkevich Method

Turkevich et al [24, 25] initiated this method in 1951. The method was subsequently improved by G. Frens in 1970 [26, 27].

Gold nanoparticles produced using this method is spherical in shape with diameters of 10-20 nm. The reaction proceeds between hot chloroauric acid with amounts of sodium citrate solution. The citrate ions act as both reducing and capping agents and are thus responsible for the formation of colloidal gold particles. A reduction in the sodium citrate content can cause the nano particles to form large particles sizes. This is because the potential for the citrate ions to stabilize the particles is limited.

2.3.2.2. Brust Method

Brust and Schiffrin came up with this method in 1990's [28]. Gold nanoparticles can be produced in organic liquids such as toluene. Tetraoctylammonium bromide (TOAB) solutions in toluene and sodium borohydride are used as anti-coagulants and reducing agent respectively. The chloroauric acid solution reacts with the reducing and anti-coagulant. Gold nanoparticles formed have about 5-6 nm [29].

The bond between the gold nanoparticle and TOAB is a weak bond. In order to prevent the particles from aggregation, thiol can be used as a binding agent to bind the gold covalently. Gold nanoparticles protected on the surface by alkanethiol can be precipitated and then redissolved Physical properties, such as solubility, can be affected when purified nanoparticles are bonded with phase transfer agent.

2.3.2.3 Perrault Method

Perrault and Chan developed this process in 2009 [30]. Hydroquinone reduces $HAuCl_4$ in aqueous solution with gold nanoparticles as seeds. The gold nanoparticles with hydroquinone can catalyze reduction of ionic gold onto their surface. Citrate can bring about controlled particle growth. The citrate method is used in producing the nanoparticles seeds. The hydroquinone method increases the range of monodispersed spherical particles sizes that can be produced. Particles produced by hydroquinone method have diameters in between 30 and 250 nm.

2.3.2.4 Sonolysis

Sonolysis is another way of producing gold nanoparticles. This process relies on ultrasound. It is a reaction which involves aqueous $HAuCl_4$ with glucose. Hydroxyl and sugar pyrolysis radicals are used as the reducing agents. The shape of particles obtained is of nano ribbons with breadth of 30-50 nm and micrometer length. The ribbons produced are flexible and can be directed into any angle. To produce gold nanoparticles of spherical shapes, cyclodextrin can be used to substitute glucose. In essence, this shows that glucose has an effect on the formation of a ribbon structure.

2.3.2.5 Martin Method

The Eah group came up with this method in 2010 [31, 32]. Gold nanoparticles were produced by reducing $HAuCl_4$ with $NaBH_4$. Even without a stabilizer, monodispersed size distribution was obtained and particle size from 3.2-5.2 nm was produced.

This formation of gold particles was possible when $HAuCl_4$ and $NaBH_4$ aqueous solutions are stabilized with HCl for a period of more than 3 months, and more than 3 hours for NaOH. Control of the ratio $NaBH_4$-NaOH ions to $HAuCl_4$-HCl ions in the sweet zone is also important in producing these particles.

A monolayer of 1-dodecanethiol is used in coating the particles produced. Moreover, it can be phase transferred to hexane by shaking a mixture of water, acetone and hexane for 30 seconds. Gold nanoparticles in the hexane phase does not need any further cleaning, since its already free. This is because all the by-products remain in the water-acetone phase. This process is fast since it takes only 10 mins. These gold nanoparticles with hydrophobic organic molecules coatings have the ability to float to the air-toluene interface to form a monolayer film. This film can be deposited to any substrate after toluene's evaporation with any simple instrument.

Phase transfer of gold nanoparticles from water to hexane and their 2D self assembly on a toluene droplet, depends on the ability to control the size diameter from 3.2 to 5.2 nm.

2.4 Gold Nanoparticles In Cancer Treatment

Introduction

Currently cancer treatment can be seen in the following; surgery/resection which is only available for each stage and small tumors, gradual giving of chemotherapy drugs to prevent the growth of cancerous cells, radiotherapy and hyperthermia [1, 2]

There are various problems associated with these methods of treating cancer. Some of these problems are outlined as follows; treatment is not localized enough and drugs cannot differentiate between healthy cells and cancer cells. Some of the specific side effects associated with the various treatment methods are; Loss of hair, damage to blood cells and damage to digestive tract in chemotherapy whereas Nausea/vomiting, diarrhea/urinary discomfort, disease in white blood cells in radiotherapy [34].

2.4.1 Nanoparticles for Cancer Detection and Treatment

Surgery, chemotherapy and radiation are the methods that are currently used in treating cancer. Physicochemical properties of the molecules are normally considered in chemotherapy. Some of

these properties include size; configuration, charge and hydrophobicity [12]. Side effects may arise in chemotherapy as a result of high drug concentration when tumor does not respond to anti- cancer drugs [13]. This may be due to changes in the biochemistry of the malignant cells, which may be the result of changes in the specific enzyme systems [13-14].

The use of nanoparticles, in conjunction with drugs, can help overcome resistance which is either cellular or non-cellular. Moreover, selectivity and potency of the drugs can be increased whiles their toxicity is minimized [15-16].

According to National Nanotechnology Initiative (NNI) [16], nanotechnology in terms of size is the dimensions involving about 1 to 100 nanometers (nm), although it could be widened to include 1000 nm. They can be made from different materials, made into varying shapes. They can also be used to transport drugs and also as a means of discovery [15]. The factors that are considered when synthesizing nanoparticles are the particle size, surface properties and the release of pharmacological active agents so as to obtain the desired location at a maximum rate and dose regimen [17].

Various materials can be used to produce nanoparticles. Some of these materials include; proteins, polymer and elements such as gold or silver. The use of a particular material depends on many factors such as required size, properties of drugs, aqueous stability or solubility, surface characteristics, degree of biodegradability, biocompatibility and toxicity and during release profiling [18].

Significant attention has been shifted to nanoparticles. This is because they are easy to synthesize. The synthesis normally involves reduction of gold salts. This may be done using capping agent molecule such as thiol, citrate and phosphine. Different chemical properties can be achieved when the functionalities are changed. Stable gold nanoparticles can be achieved when the thiol is used as its functionality. This may have many uses [19].

Gold nanoparticles can be used to detect cancer when they are attached to specific antibodies that attach to cancer cells. These include the Epidermal Growth Factor Receptor (EGFR) that attaches to receptors on breast cancer cells [20]. This is due to Plasmon Resonance.

The unique optical and magnetic properties of gold shells and iron cores can be used in the detection and treatment strategies. Gold ability to stabilize and reduce the toxicity of iron core makes it much desired [21-23]. In view of this, the gold-shelled magnetic nanostructures have many applications for target delivery, diagnosis, imaging guidance and photo-thermal ablation therapy [24]. The two possible ways of treating cancer using gold nanoparticles are explained below. These include heat treatment and drug delivery processes.

2.4.1.1 Heat Treatment

Rayleigh scattering of incident laser beams can lead, to the heating of cancer tumor in tissue in regions with nanoparticle cluster. Such heating can be controlled to achieve cell death (hyperthermia) or ablation due to laser/gold interactions. The former can be used in the treatment of cancer, while the latter can be used for the resection of tumors.

In earlier study by Karen 2010 a 250nm laser light was shone on a test tube containing gold nanoparticles. The temperatures of gold nanoparticles solution in every 30 seconds for 10 minutes were recorded. The particles used were commercially produced and were of different sizes.

It was seen that the laser light did increase the heat of the nanoparticles. The heating was most favorable at the particle size of 48nm. Again at the optimal size of 48nm, the laser heat intensities were compared. It was realized that when the laser intensity was increased the temperature also increased rapidly.

2.4.1.2 Drug Delivery

Different methods of delivering drugs have been established. These methods have been developed for both bulk systems and localized treatment of cancer. Many problems come along with the bulk systems chemotherapy, in view of this, works are been done to develop ways for localized chemotherapy. Some of the current ways of delivery systems include controlled delivery of cancer therapeutics, local chemotherapy, polymer drug conjugates, liposomal systems and transdermal drug delivery patches with possibility of the development of smart release using release microchips [35].

Conventional Drug Delivery

The amount of drugs required for effective treatment is ultimately reduced when the delivery is localized. Reduction in the side effect is therefore immense [3]. The side effect associated with bulk systematic chemotherapy can be reduced with local chemotherapy when cytotoxic is reduced. This is achieved when the drugs are delivered only to tumor cells or organs. It is also known that locally dispensing also increases the potency of the drug [4]. Tumor regrowth is greatly reduced when cancer cells are exposed continuously to drugs. This is due to an increase in the endocytosis [5, 6]. The amount of drugs used is also minimized [4, 7, 8].

Another way of treating cancer is the transdermal drug delivery [3]. The potency of protein drugs can be reduced because they have a small half life mostly during digestive processes. This is when transdermal drug delivery is used. Transdermal patches and micro needles are considered to be among the best developed delivery systems [9-11].

2.5 Adhesion mechanisms

Adhesion is the bonding of two phases on a micro or atomic scale [60]. Different ways of explaining adhesion phenomena have been proposed [60] but different theories have different systems. Various mechanisms are used in a singular case off adhesive bonding. There are five main theories and these are; mechanical, adsorption, chemical, diffusion and electrostatic. Pressure-sensitive adhesives may have pressure sensitive theories [60].

Mechanical adhesion involves the interlocking of a solidified adhesive with the roughness and irregularities of the surface of the adherent. It is mostly important on a micro scale for fibrous materials like paper and tires [61]. It has also been seen that mechanical interlocking is useful on microscopic scale [62-63].

Secondary bonds or van der Waal's forces explains adsorption theories with London dispersion forces being the well known [60]. The binding process in this theory is stated when materials are in close proximity [60]. This is because the bonding process is dependent on the presence of nuclei and electrons. The ensuing attractions are higher than the observed strength with small forces [64-65].

Diffusion theories normally takes place in polymers due to the mobility of the molecules and it involves the diffusion of macromolecules of the adhesive into the substrate or the interpretation of the molecules of each material removing the interface between them [66]. It is proven that an electrical double layer lies between metal and polymer [60]. This is the main idea behind electrostatic adhesion theory. The separation distance does not influence the force like other types of attraction. Relative changes differ at greater distances [67] as compared to others with small electrostatic forces.

Drug delivery or detecting systems that are nanoparticles based are possible because of the ability of nanoparticles to adhere to drugs and biological materials. Research have shown that the rate of adhesion nanoparticles mediated by specific adhesion molecules vary directly proportional to the receptor and ligand densities though it remains to be seen if this is common to all adhesion chemistry [58].

In the treatment of cancer using the drug delivery method, cancer drugs are attached onto gold nanoparticles. The gold nanoparticle is injected into the cancer cells. The bonds between the drugs and gold are made to break at specific pH level of the internal environment of cancer cell. The drug is released at specific target location.

Gold nanoparticle is preferred in the drug delivery method because it is easy to obtain and prepare to use. It also has high chemical stability and as such does not react easily. Gold has

affinity with thiol which are organic molecules with sulphur hydrogen (S-H) group that bridge the gold nanoparticles to drugs or other molecular recognition units (MRUs).

The drug delivery treatment is also a very specific and local treatment method. It also minimizes the effect on healthy cells.

2.6 The role of Adhesion in Nanoparticles for Drug delivery and Heat

There has been an improvement in the cancer treatment recently; however there is still challenge of diagnosis of metastasized tumor [36]. Diagnosis of cancer is often late as most of them are hidden or known metastasis [36, 37]. The death toll of cancer annually is often high whiles the experience of those who survive are often painful. They experience long and short term effects which results from surgical resection of tumors followed by bulk systematic chemotherapy; thus introduction of cytotoxic drugs in the body and sometimes radiation treatments are resorted to.

The ability of gold nanoparticles to absorb light in the visible and near-infra red (NIR) region depends strongly on the shape and size of the nanostructure [40]. Moreover, the amount of cells that can be taken gold nanoparticles is size dependent with optimal diameter of 50nm for spherical nanoparticles [41]. Great efforts have been made to produce gold composites in the detection and treatment of cancer [40, 42-50] on the basis of the interaction of gold nanoparticles and cancer cells. Such nano composites consists of an imaging case such as gold which exhibit plasmon resonance under illumination with laser; encapsulated cancer drugs like paclitaxel; molecular recognition units such as antibodies and peptides that bind specifically to receptor on cancer cells, binder/linkage chemistry and protective coatings cells that limit the interactions of the nanoparticles during transport to target organs. [70]

2.7 References

[1] Venkateswaran PS, Millman I, Blumberg BS (1987) Effect of an extract from Phyllanthus niruri on hepatitis B and woodchuck hepatitis viruses: in vitro and in vivo studies. Proc Natl Acad Sci USA 84:274–278.

[2] Rajakannan V, Sripathi MS, Selvanayagam S, Velmurugan D, Uma DM, Vishwas M, Thyagarajan SP, Shanmuga Sundara Raj S, Fun HK (2003) Phyllanthin from the plant Phyllanthus amarus. Acta Crystallogr E59:203–205.

[3] Link S, Mohamed MB, EI-Sayed MA (1999) Simulation of the optical absorption spectra of gold nanorods as a function of their aspect ratio and the effect of the medium dielectric constant. J Phys Chem B 103:3073–3077.

[4] A.P. Alivisatos, J. Phys. Chem. 100 (1996) 13226.

[5] R. Jin, Y. Cao, C.A. Mirkin, K.L. Kelly, G.C. Schatz, J.G. Zheng, Science 294 (2001) 1901.

[6] J. Aizpurua, P. Hanarp, D.S. Sutherland, M. Kall, G.W. Bryant, F.J.G. de Abajo, Phys. Rev. Lett.90(2003) 057401-1.

[7] W.M. Tolles, Nanotechnology 7(1996) 59

[8] P.R Selvakannan, S. Mandal, R. Pasricha, S.D. Adyanthaya, M. Sastry, Chem. Commun. 13 (2002) 1334.

[9] K. Okitsu, A. Yue, S. Tanabe, H. Matsumoto, Y. Yobiko, Langmuir 17 (2001) 7717.

[10] Y. Sun, Y. Xia, Science 298 (2002) 2176

[11] C. W. Corti, R. J. Holliday and D. T. Thompson, Gold Bull., 2003, 35, 111

[12] M. M. Maye, J. Luo, L. Han, N. N. Kariuki and C. J. Zhong, Gold Bulletin,

[13] M. Haruta and M. Date, Appl. Catal. A: General, 2001, 222, 427

[14] D. T. Thompson, Gold Bull., 1998, 31, 111; 1999, 32, 12

[15] D. Compton, L. Cornish and E. van der Lingen, Gold Bulletin, 2003, 36(1), 10-16; 36(2), 51

[16] D. I. Gittins, D. Bethell, D. J. Schiffrin and R. J. Nichols, Nature, 2000, 408, 67

[17] M. Shirai, K. Haraguchi, K. Hiruma and T. Katsuyama, Gold Bulletin, 1999, 32, 80

[18] M. Himmelhaus, H. Takei, Sensors and Actuators B: Chemical 2000, 63:1-2:24

[19] D. J. Maxwell, J. R. Taylor, and S. Nie, J. Am. Chem. Soc. 2002, 124, 9606

[20] T. A. Taton, C. A. Mirkin and R. L. Letsinger, Science, 2000, 289, 1757

[21] S. J. Park, T. A. Taton and C. A. Mirkin. Science 2002, 295, 1503

[22] Y. W. C. Cao, R. Jin and C. A. Mirkin. Science, 2002, 297, 1536

[23] V. R. Reddy, "Gold Nanoparticles: Synthesis and Applications" 2006, 1791, and references therein

[24] J. Turkevich, P. C. Stevenson, J. Hillier, "A study of the nucleation and growth processes in the synthesis of colloidal gold", Discuss. Faraday. Soc. 1951, 11, 55-75.

[25] J. Kimling, M. Maier, B. Okenve, V. Kotaidis, H. Ballot, A. Plech, "Turkevich Method for Gold Nanoparticle Synthesis Revisited", J. Phys. Chem. B 2006, 110, 15700-15707.

[26] G. Frens, "Particle size and sol stability in metal colloids", Colloid & Polymer Science 1972, 250, 736-741.

[27] G. Frens, "Controlled nucleation for the regulation of the particle size in monodisperse gold suspensions", Nature (London), Phys. Sci. 1973, 241, 20-22.

[28] M. Brust; M. Walker; D. Bethell; D. J. Schiffrin; R. Whyman (1994). "Synthesis of Thiol-derivatised Gold Nanoparticles in a Two-phase Liquid-Liquid System". Chem. Commun.: 801.

[29] Manna, A.; Chen, P.; Akiyama, H.; Wei, T.; Tamada, K.; Knoll, W. (2003). "Optimized Photoisomerization on Gold Nanoparticles Capped by Unsymmetrical Azobenzene Disulfides". Chem. Mater. 15 (1): 20–28. doi:10.1021/cm0207696.

[30] S.D. Perrault; W.C.W. Chan (2009). "Synthesis and Surface Modification of Highly Monodispersed, Spherical Gold Nanoparticles of 50-200 nm". J. Am. Chem. Soc. 131 (47): 17042.

[31] M.N. Martin; J.I. Basham; P. Chando; S.-K. Eah(2010). "Charged gold nanoparticles in non-polar solvents: 10-min synthesis and 2D self-assembly". Langmuir 26 (10): 7410. doi: 10.1021/la100591h. PMID 20392108.

[32] A 3-min demonstration video for the Martin synthesis method is available at you tube.

[33] Wikipedia, Electrichemistry.

[34] J. Kasthuri, K Kathiravan, N. Rajendiran (2008), Phyllantin –assisted biosynthesis of silver and gold nanoparticles: A novel approach

[35] S Douang, C. Tang, H. Zhao (2004), Photochemical Synthesis of Gold Nanoparticles by the Sunlight Radiation Using A Seeding Appraoch.

[36] M-K. Lee, S-J.Lim, and C-K. Kim. Biomaterials, 28: 2137 – 2146, 2007.

[37] S.H. Ranganath and C-H.Wang. Biomaterials, pages 1 – 8, 200

[38] M.A. Moses, H. Brem, and R. Langer. Cancer Cell, 4:337-341, 2003

[39] E.A. Ho, V. Vassileva, C. Allen, and M. Piquette-Miller. Journal of Controlled Release, 104:181 – 191, 2005.

[40] T. Herzog, R. Holloway, and G. Stuart. Gynecological Oncology, 90:45 – 50, 2003.

[41] R. Agarwal and S. Kaye. Nature Reviews, 7:502 – 516, 2003.

[42] L. Almadrones. Cancer Nursing, 26:16 – 20, 2003.

[43] P. Vasey. British Journal of Cancer, 89:23 – 2

[44] H. S.Gill, M. R. Prausnitz. J Control Release 117: 227-237, 2007.

[45] F. J. Verbaan, S. M. Bal, D. J. van den Berg, W. H. Groenink, H. Verpoorten, R. Luttge, J. A. Bouwstra. J Control Release 117: 238-245, 2007.

[46] Y. Xie, B. Xu, Y. Gao. Nanomedicine 1:184-190, 2005.

[47] R.K. Jain, Cancer Res. 47: 3039–3051, 1987.

[48] M. Links, R. Brown, Expert Rev. Mol. Med. 1: 1–21, 1999.

[49] R. Krishna, L.D. Mayer, Eur. J. Cancer Sci. 11: 265–283, 2000.

[50] I. Brigger, C. Dubernet, P. Couvreur, Adv. Drug Deliv. Rev. 54: 631-651, 2002.

[51] National Nanotechnology Initiative what is nanotechnology? [online]

Available from: **http://www.nano.gov/html/facts/whatIsNano.h**

[52] V.J. Mohanraj and Y. Chen, Tropical J. Pharm. Res. 5(1): 561-573, 2006.

[53] J. Kreuter, Nanoparticles. In Colloidal drug delivery systems, J, K., Ed. Marcel Dekker: New York, 1994.

[54] S.M. Magonov and M.H. Whangbo, Surface Analysis with STM and AFM: Experimental and Theoretical Aspects of Image Analysis, VCH Publishers, Weinheim, 1996.

[55] C.B. Prater, P.G. Maivald, K.J. Kjoller and M.G. Heaton, **www.veeco.com**.

[56] P.K. Jain, X. Huang, I.H. El-Sayed, M.A. El-Sayed, Acc. Chem. Res., 2008.

[57] M.C. Daniel, D. Astruc, Chem. Rev. 104(1): 293, 2004.

[58] M.P. Melancon, W. Lu, Z. Yang, R. Zhang, Z. Cheng, A.M. Elliot, J. Stafford, T.

[59] M.P. Melancon, W. Lu, C. Li, MRS Bulletin, 34: 415-421, 2009.

[60] K.W. Allen, Theories of Diffusion in Handbook of Adhesion by D.E. Packham, John Wiley and Sons, Inc. Hoboken, 2005.

[61] E.M. Borroff and W.C. Wake, Trans. Inst. Rubber Inst., 25: 199-210, 1949.

[62] K. Bright, B.W. Malpas and D.E. Packham, Nature 223: 1360, 1969.

[63] D.E. Packham in Aspects of Adhesion 7, Transcripta, London, 1973.

[64] R.J. Good, in Treatise on Adhesion and Adhesives, Vol 1, New York, 1967.

[65] M. Rigby, E.B. Smith, W.A. Wakeham and G.C. Maitland, Forces between Molecules, Clarendon Press, Oxford, 1986.

[66] S.S. Voyutskii, Autohesion and Adhesion of High Polymers, trans. Interscience, New York, 1963.

[67] B.V. Deryaguin and Y.P. Toporov in Physicochemical Aspects of Polymer Surfaces, Plenum Press, New York, 1983.

[68] J.B. Haun and D.A. Hammer, Langmuir, 24(16): 8821-8832, 2008.

[69] H. Karen. Gold nanoparticles in cancer treatment a comparison of adhesion forces, slides pages 4-30.

[70] Y.O. Oni, Implantable biomedical device and nanoparticles for cancer treatment.p7

[71] Lim JK, Kim Y, Lee SY, Joo SW (2008) Spectroscopic analysis of L-histidine adsorbed on gold and silver nanoparticle surfaces investigated by surface-enhanced Raman scattering. Spectrochim Acta A 69:286–289.

CHAPTER 3

3.0 GOLD NANOPARTICLES IN NANOMEDICINE

3.1 Introduction

Poor bioavailability and intrinsic toxicity are some of the problems facing conventional therapies and as a result have compromised the therapeutic efficacy of many otherwise beneficial drugs. Some of these shortcomings of the conventional therapies are been overcome by the design of nanoscopic systems to change the pharmological and therapeutic properties of molecules.

Innovative nano devices and nano structures have been produced for use in applications such as diagnostics, biosensing, therapeutics and drug delivery and targeting [1,2,3,4,5,6,7,8] In order to enhance the bioavailability of targeted site, nanosystems are often accumulated at higher concentrations than normal drugs. Systems toxicity is greatly reduced when the enhanced drug is targeted to the diseased tissue.

Moreover, drug solubility is improved when drug molecules are incorporated in nanosized systems whereas it offers a regulated release with enhanced retention at the target sites. Due to the unique properties of gold, nanosystems have been exploited to deliver drugs to target sites which are difficult to get access to such as the brain which offers serious hindrance because of the presence of the blood-brain barrier [9, 10, 11].

Gold nanoparticles are among several engineered nanoparticles that have been widely used for drug delivery, imaging, biomedical diagnostics and therapeutics applications. [1, 5, 12, 13, 14, 15, 17, 18]. As a result of their small sizes most of these nanoparticles can penetrate smaller capillaries and are taken up by the cell.

3.2 Historic Perspective in the Use of Gold Nanoparticles in the Medicine.

The use of gold in medicine has been practiced since ancient times. Small pox, slain ulcers, syphilis and measles were treated with gold in ancient Egypt, India and China [19,20,21,22]. Currently the use of gold in medicine is significant. It finds applications in medical devices such as pacemakers and gold plated stents [23] for the management of heart disease, middle ear gold implants and gold alloys in dental restoration [23]

In recent times there have been some improvements in antitumor, anti microbial, anti malaria and anti HIV activities. These are due to the emergence of several organogold complexes [21, 24, and 25]. Rheumatoid arthritis are now been treated with organogold compounds. [21, 24, and 25,26]. Even though organogold compounds can relieve arthritis symptoms such as joint pain, stiffness, swelling, bone damage and also reduce the chance of joint deformity and disability many of these compounds can show reversible dose dependent toxicities. Proteinuria and skin reactions can be experienced by the arthritis patient undergoing chrysotherapy [26]

3.3 Optical Imaging

In photoacoustic and two photon luminescence, gold nanoparticles are utilized as contrasting agents that permit light scattering and /or absorption at the NIR spectrum between 700 nm – 1000 nm [29,30]. This imaging window is known as the tissue transparency window. Light penetration at this imaging window is at maximum with minimum loss to hemoglobin and water absorption thereby permitting deep imaging of the cells [27]. In a photoacoustic experiment, Agarwal et al 2007 used 15 nm gold nanoparticles to improve cell contrast upon irradiation by a short pulse laser [30]. An ultrasonic array is used to collect the acoustic emissions created by the gold nanoparticles. This is to recreate the initial heat distribution that images the target cell.

Gold nanoparticles efficiently emit two photon luminescence because they can sustain SPR with little or no damping after the photon excitation. With appropriate delivery platforms on the gold

nanoparticles, photoacoustic and two photo luminescence imaging have been used to selectively image LnCAP prostate cancer and A431 skin cancer cells respectively [28,29,30].

3.3.1 Biosensing

Biological molecules such as antibodies, enzymes, carbohydrates and nucleic acid are used in biosensing to identify the course of any biological phenomena of interest [31,32]. Biosensors are finding use in various applications. Some of these include food processing, monitoring food – borne pathogens in the food supply, environment monitoring, detecting pollutants and pesticides in the environment, biowarfare defense to detect bacteria, viruses and biological toxins and clinical diagnostics to measure blood glucose levels [32] . The special optical and electronic properties of gold nanoparticles have been used in the sensing and /or monitoring numerous molecular events including protein-protein interaction, protein aggregation and protein folding.

3.4 Magnetic Resonance Imaging (MRI)

This is a noninvasive diagnostic tool that applies magnetic fields to the heterogenous composition of water in organisms. Different water proton relaxitivity rates translate into contrasting images of different cells [34, 35].

The MRI images can be enhanced by reducing the longitudinal and transverse relaxation time of the water proton. The enhancement is often observed by the use of contrasting agents such as gadolinium chelates or supermagnetic iron oxide [35]. The most widely used contrasting agent for MRI is gadolinium-diethyltriaaminepentaacetic acid (Gd-DTPA) [36] . In this reagent, Gd^{III} is the contrasting agent while DTPA is the chelating ligand that forms a complex with the Gd^{III} to minimize the leaching of the cytotoxic ionic Gd^{III} into the cellular milieu.

For optimal contrast enhancement, gold nanoparticles have been utilized as a delivery vehicle to convey multiple Gd-DTPA complexes into selective cellular targets. Dithiolated DTPA (DDTPA) has been utilized in place of DTPA to chelate to ionic Gd^{III} and permit conjugation

onto 2 to 2.5 nm gold nanoparticles surface. *In vivo* application and cytotoxicity of the Gd-DDTPA/gold nanoparticles conjugates have not been fully investigated [34].

3.5 Photothermal therapy

Photothermal therapy is a less insidious experimental technique that holds great assurance for the cure of cancer and related disease conditions [37]. It combines two key components which include light source and optical absorbing gold nanoparticles. The light sources are specifically lasers with a spectral range of 650–900 nm [37] for deep tissue penetration. The optical absorbing gold nanoparticles transform the optical irradiation into heat on a picosecond time scale, thereby inducing photothermal ablation.

Current developments have shown that the spectral signature of gold nanoparticles could be modified by altering their shape or size. El-Sayed and co-workers [37] have established that gold nanorods have a longitudinal absorption band in the NIR on account of their SPR oscillations and are effective as photo-thermal agents [37]. Other gold nanostructures such as gold nanoshells, gold nanocages, and gold nanospheres [38] have also demonstrated effective photothermal destruction of cancer cells and tissue. However, efficient in vivo targeting of gold nanoparticles to heterogeneous population of cancer cells and tissue still requires better selectivity and noncytotoxicity to surrounding normal cells.

.

3.6 Cancer Cell Killing: Hyperthermia with Cytotoxic Drugs

3.6.1 Introduction

Cancer therapy has many problems because it is an aggressive disease. In view of this, combined aggressive therapies are required to treat it. These include: surgery, chemotherapy, radiotherapy and hyperthermia [40, 41]. Generally, hyperthermia has been combined with various other strategies such as chemotherapy. The effects of hyperthermia on cell progression have been well studied, at least in vitro. Cell progression is impeded by hyperthermia through all phases of the cell cycle [42]. It has been revealed that mitotic divisions in untreated cells are faster than treated

cells [43, 44] and that cytokinesis is distinctly inhibited by hyperthermic treatment [43, 44]. It has also been observed that at relatively non-lethal hyperthermic treatments, cells accumulate to create partially synchronous population [45, 46]. Finally, researchers have found that hyperthermia "recruits non-cycling cells into the proliferating compartment" [42].

These studies, however, have been limited largely by some factors. First, the number of cell deaths cannot be quantified. In some instances, normal cells resisted exposure to about 43^{o}C and cancer cells were killed between 40 and 42^{o}C. However, those results could not be quantified because the survival was based on biased assessment of the rate of growth [47]. Another constraint involves the use of uncertain criteria in the assessment of cell death. These methods are either undependable or unquantifiable, as they will not show a relationship with cell death. One such method is the use of appearance, or given morphological changes, because this is more likely to vary with time after hyperthermic exposure.

A quantitative and direct relationship between loss of cell viability and inhibition of preribosomal RNA synthesis (in this case for example) has not been presented [42] even though there has been noticeable inhibition of some fundamental biochemical processes with respect to cell viability [49] . Choosing of cells for comparison is also an issue [47, 48, 50] such as comparing normal resting lymphocytes to leukemic lymphoblasts. Besides, there is still little proof that normal cells have preserved all of their normal uniqueness after exposure to heat [42, 49]. At the moment, cloning efficiency is the most reliable criterion for assessing cell death by hyperthermia. This is in the loss of the ability to reproduce in culture, or to produce tumors upon inoculation into an appropriate recipient although this method may not be applied to freshly harvested cells from normal non-tumorigenic cells [42].

With these established facts about hyperthermia, one may be able to combine this treatment modality with cytotoxic drugs in studies referred to as thermochemotherapy. The reasoning behind combining hyperthermia and chemotherapy lies with the idea that, with the right drug, synergistic effects can be achieved [51]. Although many clinical and experimental studies have been done in this regard [42], very few have tried to use both treatment methods in a way that takes into consideration the phase specificity and cell cycle progression of both modalities [3].

3.6.2 Gold Heating Of Water

By considering the measured temperature change in a water droplet containing a colloidal suspension of 20 nm gold nanoparticles after continuous wave (CW) laser excitation at 532 nm. The steady state temperature is in the interval of $28.75^0C < \Delta T < 29.25^0C$. Using the measured droplet volume of $0.0035cm^3$, the rate of constant for heat dissipation from the droplet (B) of $0.120s^{-1}$ and the laser power (I) of 0.28 W, the transduction efficiency (η) of converting absorbed light energy into heat is within the interval of $0.97 < \eta < 1.03$. [39]

The calculated η is numerically close to 1 as expected for small nanoparticles and is invariant to laser modulation. The temperature distribution inside the water droplet after laser excitation is modeled and found that on the nanoscale, the temperature profile has small bumps in temperature located around single optically simulated nanoparticles but that overall increase in temperature of the droplet is due to a collective heating effect of many nanoparticles. It is further predicted that if the particle density is reduced and a larger laser flux is used, large temperature spikes should be observed around the nanoparticles ($\sim 3^0C$) with little change in the ambient temperature ($\sim 0.2^0C$) [39].

From the experiment, the temperature trace of a $7x10^{10}$ particles/cm^3 solution of 20 nm colloidal gold nanoparticles solution drawn out in a droplet and excited with 0.28 CW laser excitation at 532 nm (fig 3.1) is shown. The droplet temperature reached steady state of ~60 s of excitation. The laser shutter was activated at this point and the decay back to the ambient temperature was followed.

The insert in fig 3.2 shows a natural log plot of $\frac{T(t)-T_O}{T_{\max}-T_O}$ as a function of time right after the laser was turned off. The temperature trace of the same droplets with different laser intensities was collected in fig 3.3. Again, the red dash line is the fit of our model to the data. The

intensities of the laser are 0.28W, 0.23W and 0.14 W. The temperature maximum in the droplet scaled with laser intensity.

The laser intensity was modulated with a chopper set before the excitation of the droplet. The temperature trace of a droplet with chopped laser intensity is shown in fig 3.4. An anisotropic square wave-waveform was applied to the laser intensity is shown in the inset in fig 3.4. The laser intensity before chopping was 0.28W. The laser was on for 2 minutes out of 5 minutes resulting in a 60% reduction in the overall laser intensity. The fit of model to the data shown as the red dash line and the different in the model fit to data is shown in the upper inset. The temperature limits in the inset is $\pm 1^0$C [39].

3.6.3 Model Energy Balance Equation

Considering energy balance equation where energy is supplied by absorption of the gold colloidal solution by the laser light (Q_i) and dissipated by transfer to an external reservoir (Q_{ext})

$$\sum_i miCp\frac{dT}{dt} = Qi - Qext \quad \text{.....(1)}$$

Where m_i, C_p, i are the mass and heat capacity components of the system, T is the temperature and t is time.

The rate of energy supplied to the system Q_i is given by

$$Q_i = I(1-10^{-A\lambda})\eta \quad \text{.....(2)}$$

Where I is the incident laser power.

A_λ is the absorbance of the nanoparticle solution

η is the efficiency of converting light absorption to thermal energy.

But

$A_\lambda = I_{opt}.\ c.\ \varepsilon$ where I_{opt} is the optical path, c is the molar concentration, ε is the molar extinction coefficient.

For the experimental situation shown in fig 1

I_{opt} = 0.186 cm; c = 1.24 x 10^{-10} mol/L; η_{np} = 7.49 x 10^{10} cm^{-3} ; ε = 9.38 x 10^8 M^{-1} cm^{-1}

The molar extinction coefficient relates to the particle cross section.

(σ_{par}) of $\sigma_{pr} = \varepsilon.\frac{10^8}{N_A}$ = 1.56 x 10^{-12} cm^2/particle. Typical number found in literature. The resulting absorbance A_λ is 0.0217.

The rate of energy flowing out of the system Q_{ext} is given by;

$$Qext = hS(T - T_0) \quad \text{.....(3)}$$

Where the dissipation energy is assumed to be proportional to a linear thermal driving force that has heat transfer coefficient h and s is the cross sectional area perpendicular to conduction. Equation 1 can be recast into a simpler form equation 4 by collecting terms and variable change.

T*, where T* is the temperature difference ($T-T_0$) from the ambient temperature T_0

$$\frac{dT^*}{dt} = A - BT^*$$

Where (A^0C/s) is the rate of energy absorption and B (s^{-1}) is the rate constant associated with heat loss.

The mass (m_w) and heat capacity ($c_{p,w}$) components of the system have been limited to just the dominant component of water forming the droplet.

$$A = \frac{Q_i}{\sum_i m_i c_{p,i}} = \frac{I(1-10^{-A\lambda})}{m_w c_{p,w}}\eta \quad \text{.....(5)}$$

$$B = \frac{hs}{m_w c_{p,w}} \quad \text{.....(6)}$$

The rate constant of heat loss from the droplet to an external reservoir is determined by following the temperature decay back to the ambient temperature after the laser excitation is turned off. In this regime, the temperature trace is given by;

$$T(t) = T_0 + (T_{\max} - T_0)\exp(-Bt) \quad \text{.....(7)} \quad when A = 0$$

Where A=0 and T_{max} is the temperature when the laser is blocked.

The steady state temperature inside the droplet is assumed to be uniform and unchanging in the droplet and is achieved when the rate of energy absorption is equal to the rate of heat loss.

The efficiency of converting absorbed light to heat (η) is extracted from the experimental curves by solving equation 9 where;

$$\Delta T = T(t \to \infty) - T_0 = \frac{A}{B}$$

And m_w, v_w and c_w are the mass and volume of the droplet and the specific heat capacity of water.

The saturation temperature measured in the experiment in fig 2 is in the interval $28.75^0C < \Delta T_{ss} < 29.25^0C$ with measuring volume of $0.0035cm^3$ $B=0.12s^{-1}$ and I=0.28W. $0.97 < \eta < 1.03$ was obtained.

The calculated η is remarkably close to 1 as expected for small nanoparticles. For larger nanoparticles we expect η to become essentially smaller than 1 due to the scattering effect. The parameter η is obtained from the following equations

$$\frac{dT^*}{dt} = 0 \text{; then } \Delta T = T_{SS} - T_0 = \frac{A}{B} = \frac{I(1-10^{-A\lambda})\eta}{B\sum_i m_i c_{p,i}} \quad \text{.....(8)}$$

$$\eta = \frac{B(T_{SS} - T_0)\rho_w c_w v_w}{I(1-10^{-A\lambda})} \quad \text{.....(9)}$$

Finally, the temperature profile after the laser is turned off is given by equation 10

$$T(t) = T_0 + \frac{A}{B}(1 - \exp(-Bt)) \quad \text{.....(10)}$$

When A≠0

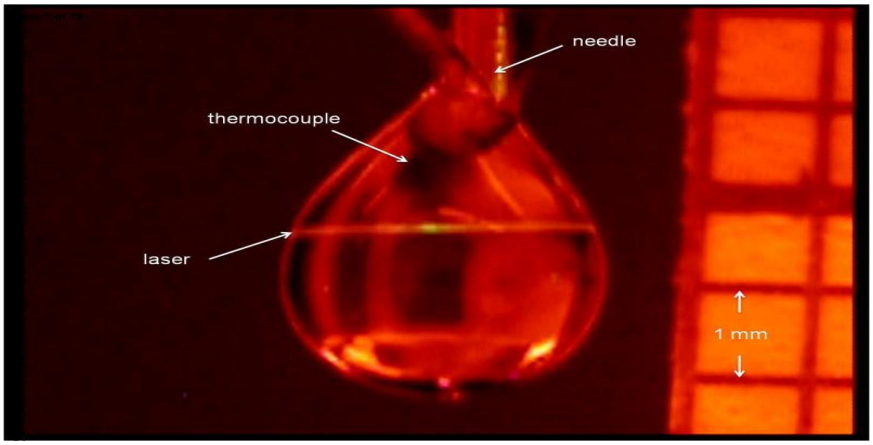

Fig 3.1 Image of typical water droplet taken during laser excitation.

The thermocouple (highlighted in the image) is embedded in the droplet. The droplet is located at the end of a stainless steel needle. The size (volume) of the droplet is determined by comparison of a grid positioned next to the droplet.

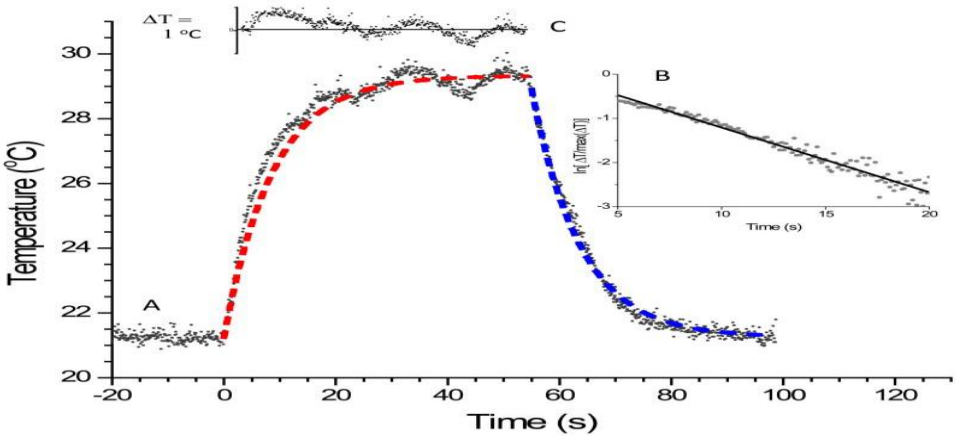

Fig 3.2 (A) Typical temperature trace showing increase in temperature after laser excitation (time = 0) and temperature decay back to the ambient after the laser is shut off (~time = 60 seconds). (B) Plot of the natural log of equation M30 as a function of time right after the laser was turned off. (C) Plot of the residual of the data compared to our model fit.I~1 [39]

The linear relationship shows that a first order decay is observed for the temperature decay back to the ambient temperature. The blue dash line in the figure is the fit of the data using the decay constant obtained from this plot. The red dash line in the figure is our model fit to the data with η equal to 1.

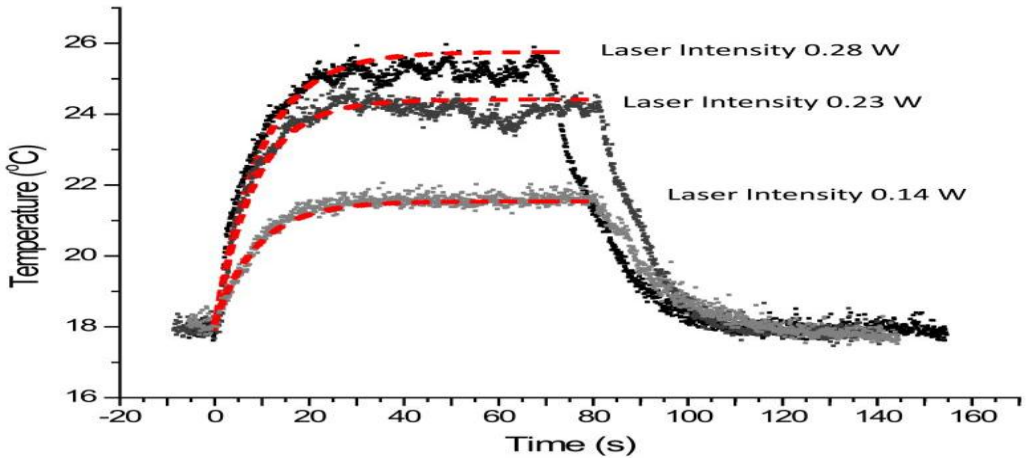

Fig 3.3 The temperature trace of the same droplet with different laser intensities.

The red dash line is the fit of our model to the data with η equal to 1. The intensity of the laser is 0.28 W, 0.23 W and 0.14 W [39].

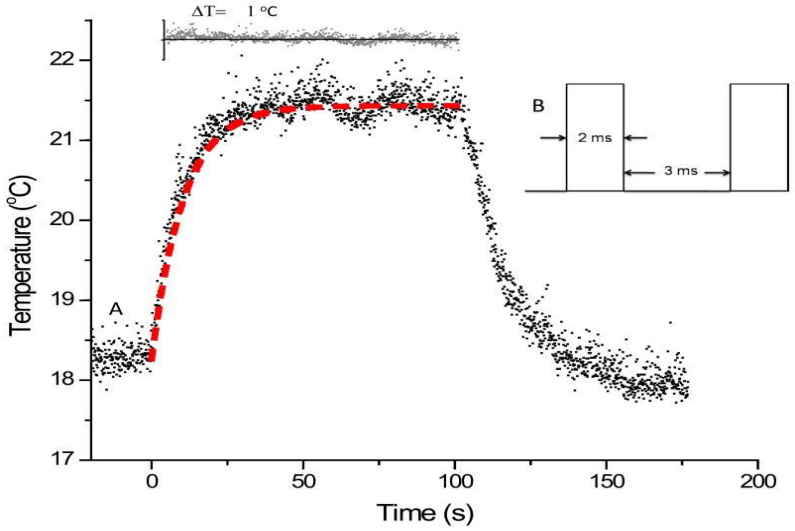

Fig 3.4 (A) The temperature trace of a droplet with chopped laser intensity.

The fit of our model to the data with η equal to 1 is shown as the red dash line. The difference in the model fit to the data is shown in the upper inset. The temperature limits in the inset is ± 1 °C. (B) An anisotropic square-wave waveform was applied to the laser intensity (originally at 0.28

W) with the resulting temperature trace shown in A. The laser was on for 2 ms out of 5 ms resulting in a 60% reduction in the overall laser intensity [39].

3.7 References

[1] Sahoo SK, Labhasetwar V. 2003. Nanotech approaches to drug delivery and imaging. Drug Discov Today, 8:1112–20.3632

[2] Freitas RA, Jr. 2005. What is nanomedicine? Nanomedicine, 1:2–9

[3] Kawasaki ES, Player A. 2005. Nanotechnology, nanomedicine, and the development of new, effective therapies for cancer. Nanomedicine, 1:101–9.

[4] Koo OM, Rubinstein I, Onyuksel H. 2005. Role of nanotechnology in targeted drug delivery and imaging: a concise review. Nanomedicine, 1:193–212.

[5] Cheng M M, Cuda G, Bunimovich YL et al 2006. Nanotechnologies for biomolecular detection and medical diagnostics. *Curr Opin Biol* 10:11-9

[6] Peters R. 2006. Nanoscopic medicine: The next frontier. Small, 2:452–6

[7] Heath JR, Davis ME. 2008. Nanotechnology and cancer. Annu Rev Med, 59:251–65.

[8] Villalonga R, Cao R, Gragoso A. 2007. Supramolecular chemistry of cyclodextrin in enzyme technology. Chem Rev, 107:3088–116.

[9] Maeda H, Wu J, Sawa T, et al. 2000. Tumor vascular permeability and the EPR effect in macromolecular therapeutics: a review. J Control Release, 65:271–84.

[10] Mu L, Feng SS. 2003. A novel controlled release formulation for the anticancer drug paclitaxel (Taxol®): PLGA nanoparticles containing vitamin E TPGS. J Control Release, 86:33–48

[11] Torchilin VP, Lukyanov AN, Gao Z, et al. 2003. Immunomicelles: Targeted pharmaceutical carriers for poorly soluble drugs. Proc Natl Acad Sci U S A, 100:6039–44.fdbch3

[12] Rawat M, Singh D, Saraf S. 2006. Nanocarriers: promising vehicle for bioactive drugs. Biol Pharm Bull, 29:1790–8.

[13] Dong S, Roman M. 2007. Fluorescently labeled cellulose nanocrystals for bioimaging applications J Am Chem. Soc, 129:13810–1.

[14] Lu C-W, Hung Y, Hsiao J-K, et al. 2007. Bifunctional magnetic silica nanoparticles for highly efficient human stem cell labeling. Nano Lett, 7:149–54.

[15] Maysinger D. 2007. Nanoparticles and cells: good companions and doomed relationships. Org Biomol Chem, 5:2335–42.

[16] Oyelere AK, Chen PC, Huang X, et al. 2007. Peptide-conjugated gold nanorods for nuclear targeting. Bioconjug Chem, 18:1490–7.7cba

[17] Skrabalak SE, Au L, Lu X, et al. 2007. Gold nanocages for cancer detection and treatment. Nanomed, 2:657–68.

[18] Cho K, Wang X, Nie S et al 2008. Therapeutics nanoparticles for drug delivery in cancer. *Chin cancer Res* 14:1310-6

[19] Huaizhi Z, Yuantao N. 2001. China's ancient gold drugs. Gold Bull, 34:24–9

[20] Richards DG, McMIllin DL, Mein EA, et al. 2002. Gold and its relationship to neurological/glandular conditions. Int J Neurosci, 112:31–53.

[21] Gielen M, Tiekink ERT. 2005. Metallotherapeutic Drugs and Metal-Based Diagnostic Agents: The Use of Metals in Medicine. Hoboken, NJ: John Wiley and Sons.

[22] Kumar CSSR. 2007. Nanomaterials for Cancer Diagnosis. Weinheim, Germany: Wiley-VCH.

[23] Svedman C, Dunér K, Kehler M, et al. 2006. Lichenoid reactions to gold from dental restorations and exposure to gold through intracoronary implant of a gold-plated stent. Clin Res Cardiol, 95:689–91

[24] Sun RW, Ma DL, Wong EL, et al. 2007. Some uses of transition metal complexes as anti-cancer and anti-HIV agents. Dalton Trans, 43:4884–92.

[25] Shaw III FC. 1999. Gold-based therapeutic agents. Chem Rev, 99:2589–600.

[26] Moolhuizen G, Paciotti GF, de Leede LGJ, et al. 2004. Colloidal gold nanoparticles. London, UK: Business Briefing, Pharmatech.

[27] Mahmood U, Weissleder R. 2003. Near-infrared optical imaging of proteases in cancer. Mol Cancer Ther, 2:489–96.

[28] Sonnichsen C, Franzl T, Wilk T, et al. 2002. Drastic reduction of plasmon damping in gold nanorods. Phys Rev Lett, 88:077402.

[29] Agarwal A. Huang SW, O'Donnell M et al 2007. Targeted gold nanorod contrast agent for prostrate cancer detection by photoacoustic imaging J Appl Phys, 102:064701-1

[30] Durr NJ, Larson T, Smith DK, et al. 2007. Two-photon luminescence imaging of cancer cells using molecularly targeted gold nanorods. Lett, 7:941–5.

[31]Otsuka H, Akiyama Y, Nagasaki Y, et al. 2001. Quantitative and reversible lectin-induced association of gold nanoparticles modified with -lactosyl – mercapto-poly(ethylene glycol). J Am Chem Soc, 123:8226–3

[32] McFadden P. 2002. Broadband biodetection: Holmes on a chip. Science, 297:2075–6.

[33] Weissleder R, Mahmood U. 2001. Molecular imaging. Radiology, 219:316–33.

[34] Debouttiere P-J, Roux S, Vocanson F, et al. 2006. Design of gold nanoparticles for magnetic resonance imaging. Adv Funct Mater, 16.2330-9

[35] Caravan P, Elhoon JJ McMurry TJ et al 1999.Gadolium (III) chelates as MRI contrast agents; structure, dynamics and applications. Chem Rev , 99: 2293-352

[36] Sharma P, Brown S, Walter G, et al. 2006. Nanoparticles for bioimaging. Adv Colloid Interface Sci, 123–6:471–8

[37] Huang X, El-Sayed IH, Qian W, et al. 2006. Cancer cell imaging and photothermal therapy in the near-infrared region by using gold nanorods. J Am Chem Soc, 128:2115–20.pj

[38] Huang X, Jain PK, El-Sayed IH, et al. 2008. Plasmonic photothermal therapy (PPTT) using gold nanoparticles. Lasers Med Sci, 23:217–28.e

[39] H. Richardson, T. Carlson, J. Tandler, P. Hernandez and O. Govorov. Experimental and theoretical studies of light-to-heat conversion and collective heating effects in metal nanoparticle solutions.

[40] B.W. Stewart, P. Kleihues, Le Cancer Dans le Monde,ed C.I.d.R.s.I.C (CIRC), IARC Press, Lyon, 2005.

[41] R. Kurzrock, M. Markman, Targeted Cancer Therapy, Humana Press, Clifton, 2008.

[42] B.K. Bhuyan, Cancer Research, 39: 2277-2284, 1979.

[43] A. Westra and W.C. Dewey, Int. J. Radiat. Biol., 19: 467-477, 1971.

[44] S.A. Sapareto, L.E. Hopwood, W.C. Dewey, M.R. Raju and J.W. Gray, Cancer Research, 38: 393-400, 1978.

[45] H.B. Kal, M. Hatfield and G.M. Hahn, Radiology, 117: 215-217, 1975.

[46] K. Kase and G.M. Hahn, Nature (Lond.), 255: 228-230, 1975.

[47] H. Vollmar, Z.Krebsforsch, 51: 71, 1974.

[48] N. Auersperg, Nature (Lond.) 209: 415-416, 1966.

[49] R. Strom, C. Crifo, A. Rossi-Fanelli and B. Mondovi, Biochemical aspects of heat sensitivity of tumor cells in: Selective Heat Sensitivity of Cancer Cells, Springer Verlag, Berlin, 1977.

[50] E.M. Levine and E.B. Robbins, J. Cell. Physiol., 76: 373-379, 1970.

[51] B. Hildebrandt, P. Wust in: W.P. Ceelen (Ed), Peritoneal Carcinomatosis: A Multidisciplinary Approach, Springer, New York, 2007, p. 185.

CHAPTER FOUR

4.0 EXPERIMENTAL PROCEDURES

4.1 Biosynthesis Of Gold Nanoparticle

4.1.1 Isolation Of bacteria in the soil

The bacteria used locally were isolated from the soil in Gwagwalada town in Abuja, Nigeria.

The equipments and materials used in the experiment include the; 10 Mml beakers, conical flasks, micropipette, micropipette tips (sterile), Bijou bottles containing 9ml of sterile distilled water, normal sterile saline water, Laminar flow hood, (Biosafety Cabinet Model 36204/36205 TYPE AZ) bunsen burners, an autoclave, Incubator, a shaker incubator (Innova 44 Incubator series) 70% ethanol and L shaped spreader Petri dishes.

4.1.2 Serial Dilution

Bijou bottles containing 9 mls of distilled water were autoclaved to sterilize the water. Subsequently, 1g of the soil sample was weighed and dissolved in 10 mls of water. The mixture was then stirred thoroughly using a stainless steel stirrer. Then 1 ml of each dissolved sample was added to the first Bijou bottle and made up to 10 ml, before stirring thoroughly. 1 ml was taken to the next until it reached the last bottle and the solution was observed to gel clear in each dilution. 0.1 ml of the last diluents was inoculated in well labeled nutrients agar media respectively in a spread plate fashion. After inoculation, the plate was kept in an incubator for growth of the microorganisms.

Serial dilution was done to reduce the colonies that would appear in each plate for easy quantification. A spread plate method was used instead of pour plate method in order to give more room for both aerobic and anaerobic microorganisms to grow. Every material or tool used for the experiment was constantly sterilized to ensure that only microorganisms from the soil

samples were inoculated. After the experiment, the glass wares were washed and allowed to dry in the oven.

4.1.3 Preparation of MacConkey Agar, Peptone Glycerol Agar and Luria Bertani (Lb)

4.85 g of MacConkey agar was dissolved in 100 ml of distilled water in a conical flask. The solution was divided into four equal volumes of 25 ml with a syringe into test tubes. They were dispensed before autoclaving at $121^{O}C$ for about 15 mls.

0.5g of peptone, 1 ml of glycerol and 1.5 g of agar were mixed and dissolved in a 100 ml of distilled water in a conical flask. The solution was dispensed into four equal volumes of 25 ml with a syringe into test tubes. They were also dispensed before autoclaving at $121^{O}C$ for about 15 mls.

3.7 g of Luria Bertani was dissolved in 100 ml of distilled water in a conical flask. The solution was divided into four equal volumes of 25 ml with a syringe into test tubes. They were dispensed before autoclaving at $121^{0}C$ for about 15 mls.

All the 12 samples were grouped in three different bottles, and labeled accordingly, to prevent specimen mix-up. They were autoclaved to sterilize them. After autoclaving, the test tubes were slanted and allowed to rest for about 48hrs. This resulted in sample cooling and solidification.

4.1.4 Preparation of Pure Culture

Pure cultures were used to identify unique microorganisms obtained from the various colonies. These unique microorganisms were then used in determining the bacteria that are suitable for the synthesis of the gold nanoparticles.

Nutrient agar was used in the sampling of the various bacteria in the environment. The nutrients that are needed by bacteria to grow include sugars, amino acids, vitamins, minerals and a carbohydrate from marine algae. These are found in nutrient agar. A bacterial cell taken from the soil and placed on the surface of a NA (nutrient agar) plate, can multiply into a colony of cells visible to the naked eye. MacConkey agar is also used to grow Ecoli that are readily visible to the naked eye.

4.1.5 Media Preparation for Bacillus Subtilis and Bacillus Megaterium

Nutrient agar and nutrient broth were prepared for bacillus subtilis and bacillus megaterium that were obtained from Dr. Karen Malatesta of Princeton University.

The nutrient agar contained beef extract 3 g/l; Peptone 5 g/l; agar 12 g/l and NaCl 5 g/l. A solution of 2.8g of nutrient agar in 100 ml of distilled water was prepared at a pH of 7. Pre-gelling was initially done to avoid the solution solidifying into 2 layers after autoclaving.

Autoclaving was done afterwards for sterilization. The solution was poured onto petri plates and left overnight so that they could form a uniform gel which could be used in inoculating. This is done in a laminar flow loop as a means of getting rid of outside microorganisms.

The contents of the nutrient broth were beef extract 1.5 g/l; Peptic digest of a tissue 5 g/l; yeast extract 1.5 g/l. A solution of 1.3g of nutrient broth in 100ml of distilled water was prepared at a pH of 7. The solution was dispensed into 10 bijou bottles. This was done to maximize the small quantity of the microorganism by growing on it. Autoclaving was done afterwards for sterilization. This is done in the laminar flow loop as a means of getting rid of outside microorganisms.

To confirm that the bacteria were single colonies of Bacillus megaterium and subtilis, they were made into broth then into plates and sent back to broth again so that they can increase in population.

Three different microorganisms were considered for the biosynthesis. The three were chosen after various tests were performed on them to see which of the microorganisms isolated were capable of producing gold nanoparticles. The three bacteria include Bacillus subtilis, Bacillus megaterium and serratia mercenses mercenses isolated from the soil.

Nutrient broth solution was prepared so that the population of the various cells would be increased. This was to enable us acquire large quantity of individual cells for the biosynthesis. 1.3g of nutrient broth was dissolved in 100 mls of distilled water in all four cases. 1% of glucose was added to the solutions as a supplement for the microorganisms. Autoclaving was done to kill all unwanted bacteria in the solutions and its surroundings. All the three microorganisms were

inoculated into the solutions in aseptic conditions in a laminar flow hood. The samples were placed in a shaker incubator (Innova 44 Incubator series) for 48 hours at $32^{O}C$ for the growth of the microorganisms.

In order to monitor the growth of the microorganisms on plates, a solution of the gold solution and nutrient agar was prepared. The solution which contained 2.24g of nutrient agar was dissolved in 80 mls of distilled water was autoclaved to kill all unwanted bacteria. Inoculating of the various bacteria was done in an aseptic condition in a laminar flow hood (Biosafety Cabinet Model 36204/36205 TYPE AZ). The three bacteria that were used in the biosynthesis of the chloroauric salt were serratia mercensis mercensis, Bacillus megaterium and Bacillus subtilis.

4.1.6 Experimental Procedure

Materials needed for the experiment include the following,

Photosynthesis bacteria, Medium for bacteria. Nutrient broth, Sodium hydroxide (NaOH) and hydrochloric acid (HCl), Centrifuge, Carbon coated grid, Aurochloric acid ($HAuCl_4$) and UV visible spectrometer.

The medium used to culture the photosynthetic bacteria consisted of beef extract 1.5 g/l; Peptic digests of a tissue 5 g/l; yeast extract 1.5 g/l is used to culture the photosynthetic bacteria. The pH was set at 7 with a temperature of $30^{O}C$. These conditions are set for the growth and survival of the bacteria.

The culturing process was carried out for 72 hours. After centrifugation at about 3000 rpm at $4^{0}C$ for 10 minutes, the bacteria were separated from the other components of the medium. Distilled water was used to wash the separated bacteria from the other chemicals of the medium. The washing was done about 5 times. A wet weight of about 1 gram of the bacteria was measured. This was then suspended in an aqueous aurochloric acid ($HAuCl_4$) in a test tube of concentration $1x10^{-3}M$ aqueous and of volume 20 mls. A NaOH solution of concentration 0.1M was used to neutralize the reactants to a neutral pH.

In other experiments, the starting pH of the mixture of $1x10^{-3}M$ $HAuCl_4$ solution and biomass was adjusted to 3 and 7 using 0.1 M HCl and NaOH solutions, respectively in test tubes. All experiments were conducted at room temperature for a period of 48 hours.

A UV-visible spectrophotometer was used to measure the UV- visible spectra of the nano particles that were formed after the 48 hour exposure.

4.2 Role Of Adhesion In Nanoparticle

4.2.1 Experimental Procedure

Materials used in the experiment by Oni et al [1] are the breast cancer cell line; MDA-MB-231, growth media (L-15), and medium supplements (fetal bovine serum and penicillin/ streptomycin) were purchased from American Type Culture Collection (ATTC, Manasses, VA). Dubelcco's Phosphate Buffer Saline (PBS) was obtained from Invitrogen (Carlsbad, CA) and formaldehyde solution, triton X-100, 0.1M sodium hydroxide; BSA, dibasic sodium phosphate buffer and monobasic sodium buffer were all obtained from Sigma-Aldrich (St. Louis, MO). The gold nanoparticles were Nanopartz Inc. (Loveland, CO) while the uncoated AFM tips were brought from Veeco (Memphis, TN). Paclitaxel was obtained from Parenta Pharmaceuticals (West Colombia, SC), LHRH was purchased from Thermo Scientific (Waltham, MA) while Breast Specific Antibody (BSA) were obtained from Sigma-Aldrich (St. Louis, MO) [1].

4.2.2 AFM Experiments

4.2.2.1 Tip Coatings

A simple coating method was employed [8]. In this method bare AFM tips were coated with the gold nanoparticles about 10-15 times between 2-4 seconds interval. Gold nanoparticles concentrations of 22-46 ppm were used depending on their sizes and were utilized as received condition. The coated tips were dried in air for a minimum of one day and observed under a scanning electron microscope [1].

4.2.2.2 Tip Characterization

A Phillips model FEI XL30 field emission gun scanning electron microscope (SEM) (Phillips Electronic N.V. Eindhoven, The Netherlands) was used to observe the AFM tip samples coated with gold nanoparticles and the bare tips. Images obtained were from the secondary electrons from the samples. Images of coated tips were taken before and after the AFM experiments to make sure that the measured adhesion forces of the nanoparticles with the cells are the true values. This was done because the dip-coating process results in poor adsorption [1].

Thermal tune method was used to measure the spring constants of the coated and uncoated tips [12, 13]. To obtain the true adhesion forces from equation 6.1, the actual spring constant are required. This also accounts for batch-to-batch variations in the spring constants, as well as the effects of coatings on the cantilever stiffness [8, 11]. The pull off measurements was obtained under ambient condition at room temperature of 22-23^{O}C and a relative humidity of 40-45% [1].

4.2.2.3 Cell Substrate Fixation

Prior to use as substrate in the AFM experiments, the cells were fixed against the tips. Initially the breast cancer cell lines used were cultured on glass slides (MatTek, Ashland, MA) until they were fully confluent. The cells were incubated at 37^{O}C at atmospheric pressure and grown in L-

15 growth medium. There were supplement with 10% FBS and 100 I.U./ml penicillin/ 100µg/ml streptomycin.

The cells were washed twice with glacier PBS solutions (1XPBS at $4^{O}C$) and fixed with 15 minutes incubation with 3.7%, formaldehyde solution once the desired confluence level was attained. The fixed cells were further rinsed with glacier PBS three fines, followed by three rinses with distilled deionised water. Water was used as the medium for the last rinse to remove possible salts deposits that may have resulted from the prior PBS rinses. Lastly the fixed cells were dried in a vacuum dessicator for two hours.

4.2.3 Atomic Force Microscopy Measurements.

A stable nanoparticle based nano composite is required for the transportation in the body. Adhesive interactions are measured among the various compositions. Atomic force microscopy (AFM) is an approach that can be used. [2]. AFM can be used to measure the interaction between nanoparticles. This can be done by coatings AFM tips by bringing them close enough with coated substrates that can behave as pair wise interactions between interacting nanoparticles [3].

There are steps involved in the AFM methods

The AFM tips are brought close enough for the adhesive interactions. There is a jump into contact. The tips undergo elasticity due to further displacement in the same direction. The effects of adhesion do not allow the tip to detach as zero loads. Retraction is continued till the applied forces are sufficient to pull off the AFM tips from the substrates. The resisting pull off force, F is a measure of the adhesion. It can be obtained from Hooke's law which is F= k d.

Where k is the stiffness of the cantilever d is the displacement at the onset of the pull off.

The difference between breast cancer cells and normal breast cells has been detected as a result of the measurements of such pull off forces [4-8]. Meng et al studied the adhesive interactions between the $EphA_2$ antibody and receptor on breast cancer or normal breast cancer as well as the adhesion between the luteinizing hormone releasing hormone [LHRH] peptides and their receptor on breast cancer and normal breast cancer.

Their results showed that the pull off force associated with breast cancer cells and LHRH EphA2 which are over expressed in breast cancer cells [9, 10] are about 5 times those with normal breast cells [8]. Force microscopy can therefore be used to detect cancer cells in vitro.

AFM will thus be used to obtain the adhesion forces between gold nanoparticles, cancer drug paclitaxel and cancer specific antibody or LHRH for detecting/deliver strategy.

4.2.4 AFM Force Displacements Measurements.

A Multimode Dimension DI Nanoscope IIIa Atomic force Microscope (Veeco Instruments, Woodbury, NY) was used to measure the interactions between the gold nanoparticle-coated AFM tips and the cell substrates or between the components of the drug delivery. This was done at ambient conditions at room temperature (22-23^{O}C) and relative humidity (40-45%).

Calibration of the photo detector sensitivity on the stiff quartz surface was done before force microscopy measurements [14]. Average of 150 measurements obtained from 3 tips thus 50 measurements were obtained for each tip at five different positions.

4.3 Gold Heating of Water

Experiment Procedure

In an experiment conducted on gold heating of water, gold nanoparticle concentration of $7x10^{10}$ particles/cm^3 was used. Approximately 10 µL of the solution was extricated from the syringe to maintain a stationary hanging drop on the tip of the needle, fully submerging the thermocouple bead inside the sample drop [10].

The laser was aligned to pass through the drop without hitting the thermocouple. As the laser irradiated the sample, the temperature began to increase. Data was collected until equilibrium temperature was reached. Using the equation of an ellipsoid, the volume of the drop was

approximately determined. The path length of the laser through the drop was also determined from the captured video [10].

4.4 References

[1] Y.O. Oni, Implantable biomedical device and nanoparticles for cancer treatment.p155-171

[2] S. N. Magonov and M.-H. Whangbo, Surface Analysis with STM and AFM: Experimental and Theoretical Aspects of Image Analysis ⁄VCH, Weinheim, 1996.

[3] C. B. Prater, P. G. Maivald, K. J. Kjoller, and M. G. Heaton, www.veeco.com.

[4] P. Hinterdorfer, G. Schütz, F. Kienberger, and H. Schindler, Rev. Mol. Biotechnol.

82: 25, 2001.

[5] V. Dupres, F. D. Menozzi, C. Locht, B. H. Clare, N. L. Abbott, S. Cuenot, C.

Bompard, D. Raze, and Y. F. Dufrene, Nat. Methods 2: 515, 2005.⁄

[6] E. Wojcikiewicz, X. Zhang, and V. Moy, Biol. Proced. Online 6: 1, 2004.

[7] Li, S. D. Redick, H. P. Erickson, and V. T. Moy, Biophys. J. 84: 1252, 2003.

[8] J. Meng, E. Paetzell, A. Bogorad, and W. O. Soboyejo, J. Appl. Phys. 107: 114301, 2010.

[9] W.R. Miller, W.N. Scott, R. Morris, H.M. Fraser and R.M. Sharpe, Nature 313: 231 – 233, 1985.

[10] H. Richardson, T. Carlson, J. Tandler, P. Hernandez and O. Govorov. Experimental and theoretical studies of light-to-heat conversion and collective heating effects in metal nanoparticle solutions.

CHAPTER FIVE

5.0 RESULTS AND DISCUSSIONS

5.1 Biosynthesis of Gold nanoparticles

Three bacteria namely Serratia mercensis mercensis, Bacillus megaterium and Bacillus subtilis were used in the synthesis.

Upon exposing the three bacteria to the aqueous chloroauric ions, the bacteria were able to reduce the aqueous chloroauric ions to gold atoms. The colour of the solutions changed from yellow to dark purple for serratia mercensis mercensis and bacillus megaterium and from bacillus subtilis to purple (as shown in the fig). The reactions were completed after minimum of two days and they gave an idea of slow reaction processes. The dark purple colour change remained the same and the gold nanoparticles were analyzed by UV-Vis spectra.

Other experiments were done to confirm whether the addition of the various microorganisms were responsible for the reduction of the chloroauric ions. It was observed that the colour of the chloroauric ions stayed yellow when microorganisms were not added to the solution for the same time period.

The UV-Vis absorption spectra obtained from the gold nanoparticles solution after two days of reaction for the three bacteria are shown below. At a pH of 3, the absorption was maximum at 260 nm for serratia, while B. megaterium and B. subtilis gave maximum absorbance at 430 nm and 372 nm respectively. There were slight absorptions at around 530 nm for the three bacteria. The absorptions at these wavelengths were not maximum and these can be attributed to the fact that the nanoparticles were occluded by some proteins which were excreted by the bacteria in the various solutions. At a pH of 7 the absorption was maximum at 264 nm for serratia, while B. megaterium and B. subtilis gave maximum absorbance at 266 nm and 262 nm respectively. There was absorption at around 530 nm for serratia whiles B. subtilis and B. megaterium

recorded absorptions at 535 nm and 544 nm respectively. The absorptions at these wavelengths were also not maximum and these can be attributed to the fact that the nanoparticles were occluded by some proteins which were excreted by the bacteria in the various solutions. As a result of the supposed proteins occluding the nanoparticles, absorption maximum at around 540nm attributed to the surface plasmon resonance band (SPR) of the gold nanoparticles was not achieved.

The stability of the gold nanoparticles can be tested. This can be done by filtering the gold nanoparticles from the various microorganisms. The solution obtained after the filtration can be aged for not less than three months. UV-Vis spectra measurement can thus be used in determining the stability of the gold nanoparticles [1]. Experiments were performed to detect the viability of the various bacteria to the gold ions and gold nanoparticles. The various bacteria proliferated when small drops of solution containing the bacteria when inoculated on agar plates. This showed that the bacteria are resistant to the gold ions and gold nanoparticles.

The particle sizes of the various nanoparticles produced by the bacteria can be determined by transmission electron microscopy (TEM). It can be predicted that the pH was an important parameter in the gold nanoparticle synthesis in all the three cultures. Variations in the pH from 7 to 3 gave visual evidence in colour changes from light purple to dark purple. This could mean that the pH has an impact on the size, shape and the number of particles produced. It can also be predicted that the shape of particles produced at pH of 3 will be mostly spherical and relatively uniform in size. However, particles produced at pH 7 will include small spherical particles with bigger particles which are irregular in shapes. These predictions are supported by previous works suggesting that optimum gold accumulation of by microbial cells normally occurs in the pH range of 2-6 [5]. The changes in the shape of particles formed at the two pH levels shows changes in the pH would play an important role during optimization of a process controlling particle morphology [6]

5i)  5ii)  4iii) 

Fig 5.10 (A) Pictures show various bacteria (B. megaterium, B. subtilis and Serratia) growing on a solution of gold and agar plates formed as gels.

(5B) Serratia mercensis mercensis

5.11a)  5.11b) 

Fig 5.11 Picture of tubes containing bacteria serratia mercensis mercensis before (tube 5.11a) and after 72 hrs (tube 5.11b) in an aqueous of $AuCl^-_4$

(5.12a) 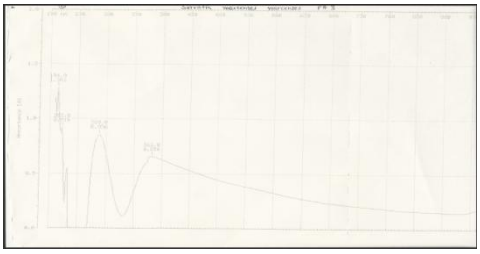 (5.12b) 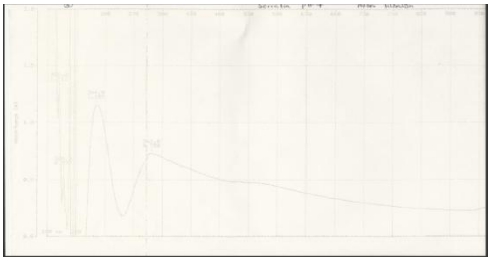

Fig 5.12 shows UV-Vis absorption spectra of gold nanoparticles after reaction of 10^{-3}M aqueous $HAuCl_4$ solution at neutral pH and pH at 3 with the bacteria serratia mercensis mercensis

(C) Bacillus megaterium

5.13a) 

5.13b) 

Fig 5.13 Picture of tubes containing bacteria Bacillus megaterium before (5.13a) and after 72 hrs (5.13b) in an aqueous of $AuCl^-_4$

(5.14a) 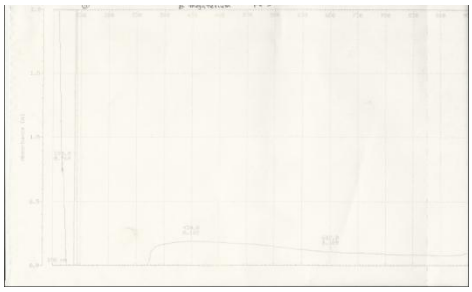

(5.14b) 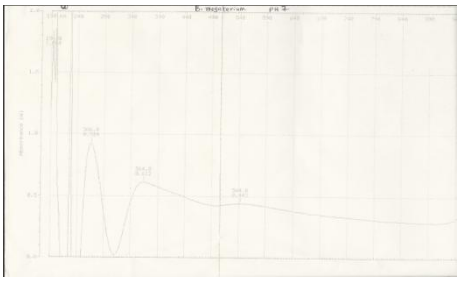

Fig 5.14 shows UV-Vis absorption spectra of gold nanoparticles after reaction of 10^{-3}M aqueous $HAuCl_4$ solution at neutral pH and pH at 3 with the bacteria Bacillus megaterium

(D) Bacillus subtilis

5.15a) 

5.15b) 

Fig 5.15 Shows Picture of tubes containing bacteria Bacillus subtilis before (tube 5.15a) and after 72 hrs (tube 5.15b) in an aqueous of $AuCl^-_4$

(5.16a) 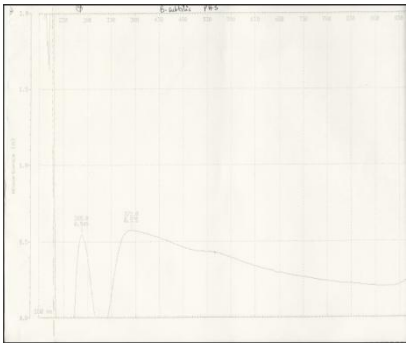 (5.16b) 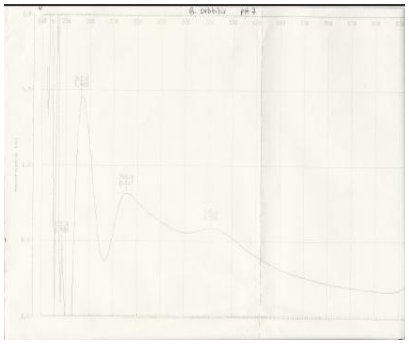

Fig 5.16 shows UV-Vis absorption spectra of gold nanoparticles after reaction of 10^{-3}M aqueous $HAuCl_4$ solution at neutral pH and pH at 3 with the bacteria Bacillus subtilis.

5.1.1 Conclusions and Future Works

In conclusion, it has been demonstrated that the bacteria B. megaterium, B. subtilis and serratia mercensis mercensis are able to produce gold nanoparticles and the gold nanoparticles are quite stable in solution. This is an efficient, eco-friendly and simple process. The shapes of the gold nanoparticles produced by the three bacteria were controlled by pH. Work is continuing for the study of the biological mechanism for the nanoparticles formation and more detailed study of controlling the shapes and sizes of nanoparticles. The NIR absorbance of the gold nanotriangles could find interesting applications in cancer hyperthermia. This work will also lead to the development of a rational biosynthetic procedure for other metal nanomaterials such as silver and platinum with the bacteria B. megaterium, B. subtilis and serratia mercensis mercensis.

5.2 Measurement of Adhesion forces

Adhesion forces obtained for coated tips are different from bare tips. Coated tips have particles on the sides whiles bare tips are evenly smooth on the side and along the surface of the cantilever. This can be seen in fig 5.4 and 5.5

Fig 5.6 shows the interactions between the different composites of the drug delivery systems. It can be seen that the adhesion forces between the gold nanoparticles are comparable and stronger than those obtained for paclitaxel- LHRH complexes.

The results obtained are significant. Initially the results give an indication that the drug gives rise to the weakest adhesive interactions within the drug nano composite system. Paclitaxel gives a pull off force of about 10 nN compared with those without the drug (F~ 58 nN). The implication of this result is that the cohesive forces between the drug is stronger and that robustness of such systems will depend highly on the drug composites interactions.

Moreover, the fig 5.6 shows that the attraction to biological compounds by gold is very strong with gold recording pull off forces of about 60±5, 57±3 nN for gold- LHRH and gold-AB respectively. They are far better than between gold and paclitaxel which is 11±0.5 nN. This confirms the studies that gold has an excellent biocompatibility [3].

It can also be seen that the attractive interactions between paclitaxel and molecular recognition units, LHRH and antibody is weak 10±1 nN and 9±1 nN are the pull off forces obtained which are less than the other interactions within the system. Again it can be observed that since the drug is the weakest in the system, careful engineering is to be done to prevent its release before it is required.

Fig 5.7 shows the interactions forces between each nanoparticle size measured against breast cell substrates. For radius between 30nm, the adhesive forces were optimal. The results show that there is a strong adhesive force for gold nanoparticles of about 30nm. This pull off force then closes to breast cancer cells.

The plot of fig 5.7 reveals how the receptor of breast cancer cells and nanoparticles interact using the AFM.

Fig 5.8 also reveals the interactions between thiol, gold and drug/molecular recognition units. It can be seen that, the adhesion forces between gold and thiol is optimal at 113±1 nN and maximum at 319±1 nN for antibody and thiol. However, for a bare tip gold interaction and bare tip thiol interaction, the adhesion forces are 23±1 nN and 9±1 nN respectively. Thiol therefore affects the adhesion forces between gold and drug/molecular recognition units in such a way that it can bridge the gold particles well with drugs to prevent unwanted release of the drug.

5.2.1 Conclusions and Future Works

This work has investigated the adhesion between components of a model generic drug delivery/system that includes gold nanoparticles, paclitaxel and over-expressed protein in breast cancer, LHRH or breast-specific antibody. The results imply that the robustness of such systems depends on the adhesion with the paclitaxel. In such cases, it is important to design systems such that bonding with the drug is increased to prevent unwanted release. The results also suggest that the force microscopy technique can be used to rank the adhesion between different species in drug nanocomposites that are being developed to treat breast cancer and other forms of cancer. It was also revealed that thiol affects the adhesion forces between gold and drug/molecular recognition units. The current work also shows that gold nanoparticles with sizes of ~30 nm are optimal in terms of their adhesion to human breast cancer cells (MDA-MB-231) examined in this study. Further work is needed to measure the adhesion forces in biological environments.

5.3 Nanomedicine

Concerning the work on nanomedicine, some of the current applications of gold nanoparticles in nanomedicine have been reviewed. Small molecules, peptides, and proteins are some of the assorted collection of gold nanoparticles delivery strategies that are under study. These have shown great promise in specific targeting of gold nanoparticles to diseased tissues. Moreover, the biocompatibility and photo-optical distinctiveness of gold nanoparticles are now demonstrated to be powerful in diagnostic and biosensing applications. This therefore offers a bright hope for the diagnosis and treatment of many disease states.

The continued attraction of the scientific community with gold nanoparticles research have been facilitated by significant strides in many fronts including availability of many methods for the production and functionalization of gold nanoparticles of various shapes and sizes. It is now possible to control particle sizes at nanometer resolution. Enhanced understanding of molecular targeting in biology has provided several ligands that have been successfully used for specific delivery of gold nanoparticles. With information ensuing from proteomics studies on various diseases, one expects that many more ligands will be made available for gold nanoparticles-targeted delivery.

However, the successful implementations of the promised applications of gold nanoparticles are still limited in part by the formidable barriers imposed by the complexity of a whole organism in contrast to simple cell based studies that formed the bed rock of most of the proof-of-principle investigations. There are important evidence that gold nanoparticles-based therapeutic agents could rise above the difficulties presented by the human immune and circulatory systems to achieve delivery at diseased sites without uptake by healthy tissues. In principle, such improved targeted delivery could make other gold nanoparticles-based experimental therapeutic techniques, such as photothermal therapy, feasible. With the right combination of delivery agents and particle size, gold nanoparticles-based therapeutics could in actual fact kill unhealthy cells while removing the terrible side effects of the conventional chemotherapeutic agents.

5.3.1 Conclusions and future works

More work still needs to be done regarding the understanding of the pharmacokinetics and toxicity profiles of gold nanoparticles. Particular interest should be given to gaining comprehensive insights on the effects of nanoparticle size, ligand conjugation and conjugation chemistry on gold nanoparticles physiological properties. Additionally, the prospective for cumulative toxicity upon repeated exposure to gold nanoparticles based agents must be carefully examined. Nanotoxicity may not be a small matter after all. Results from these and related studies will prove informative in further improvement of the design of gold nanoparticles for use in diverse nanotechnology applications.

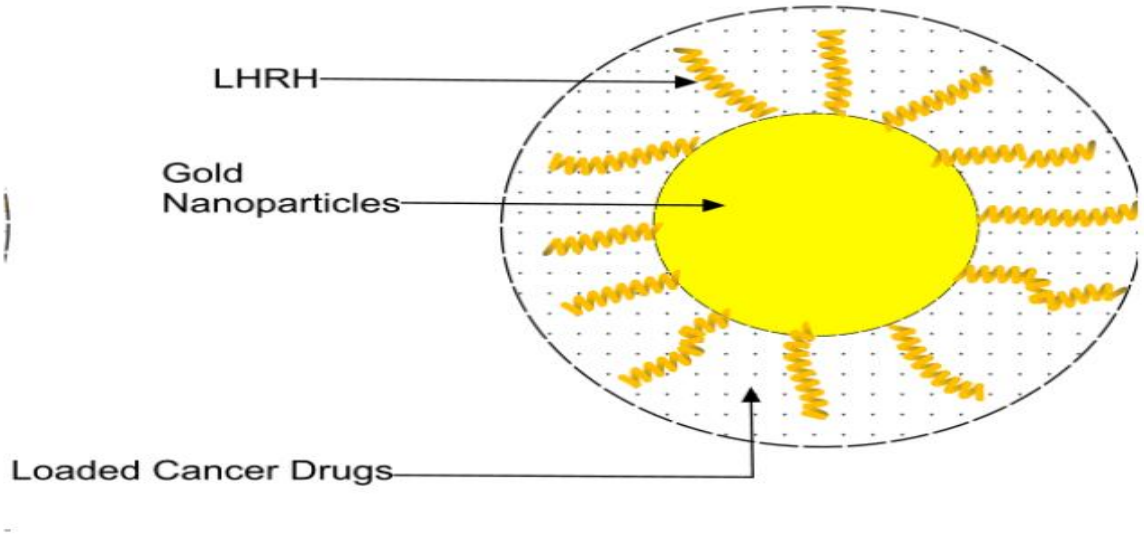

Fig 5.2 Schematics of a nanoparticle-based drug delivery/detection system © Y. Oni 2010

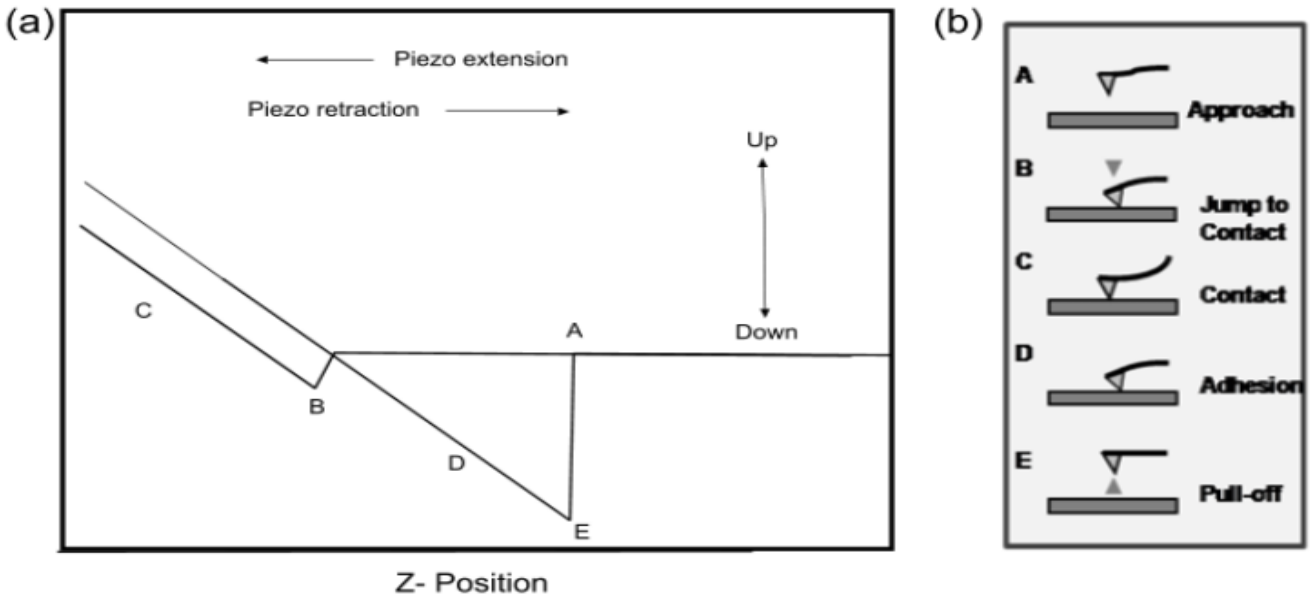

Fig 5.3 Schematics of force spectroscopy techniques: (a) typical force-displacement plot, (b) corresponding physical scenarios. © Y. Oni 2010

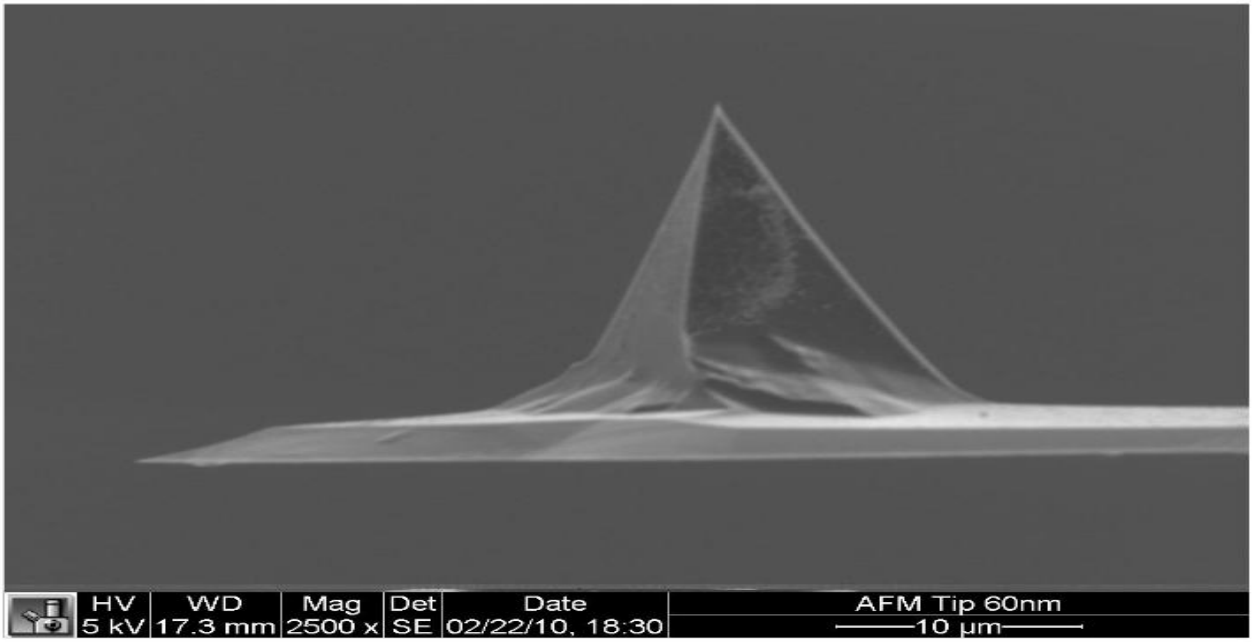

Fig 5.4 SEM image of a coated tip. © Y. Oni 2010

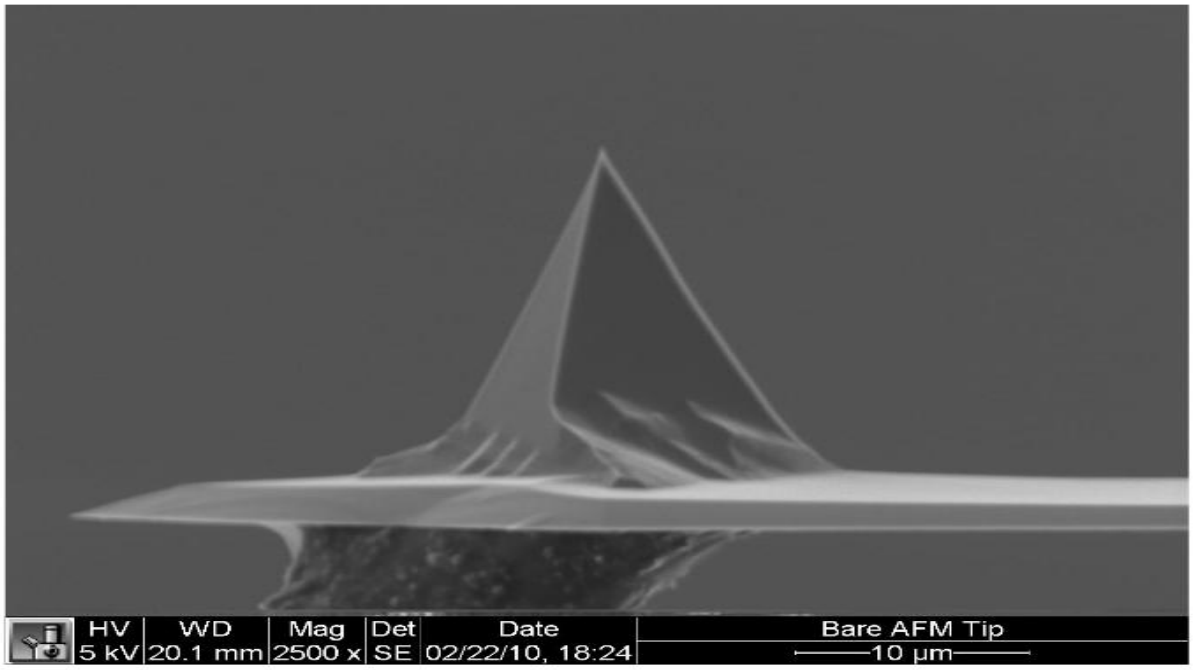

Fig 5.5 SEM image of a bare tip. © Y. Oni 2010

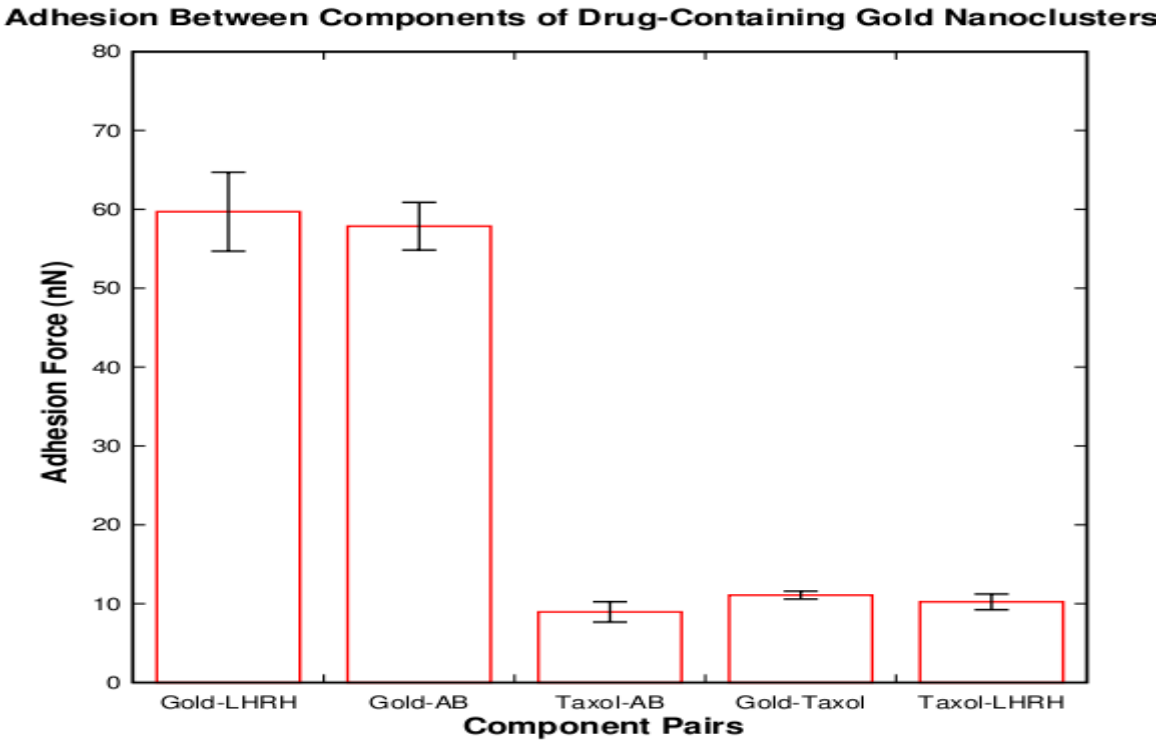

Fig 5.6 Adhesion interactions of components in a drug delivery system © Y. Oni 2010

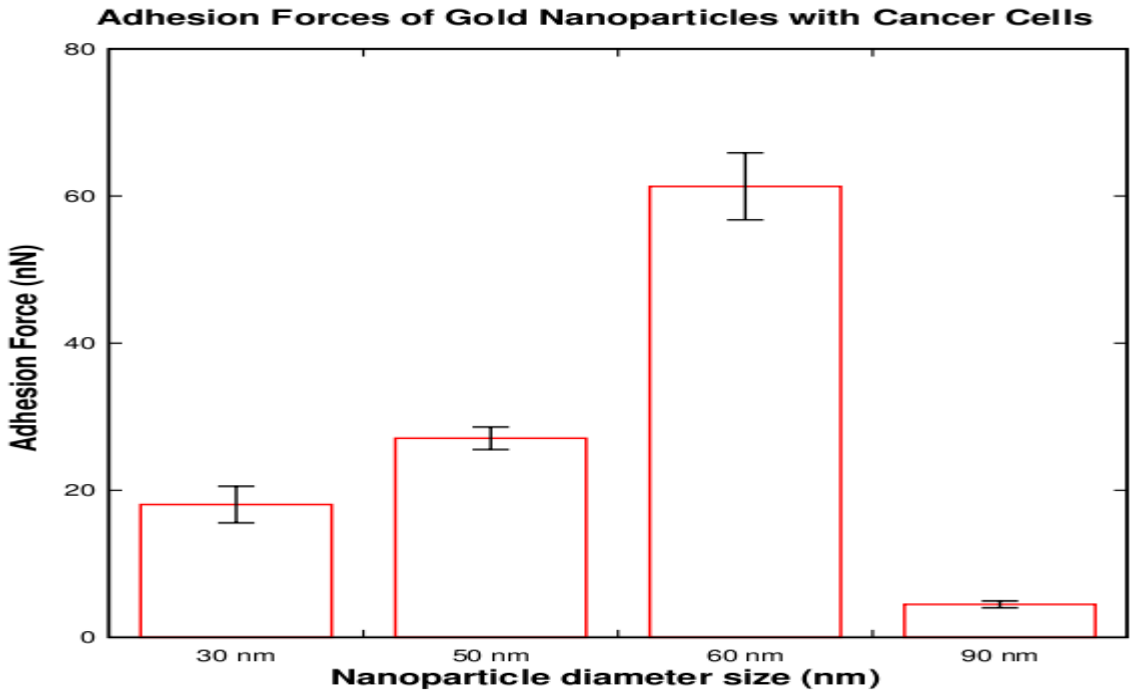

Fig 5.7 Adhesion forces of gold nanoparticles with breast cancer cells © Y. Oni 2010

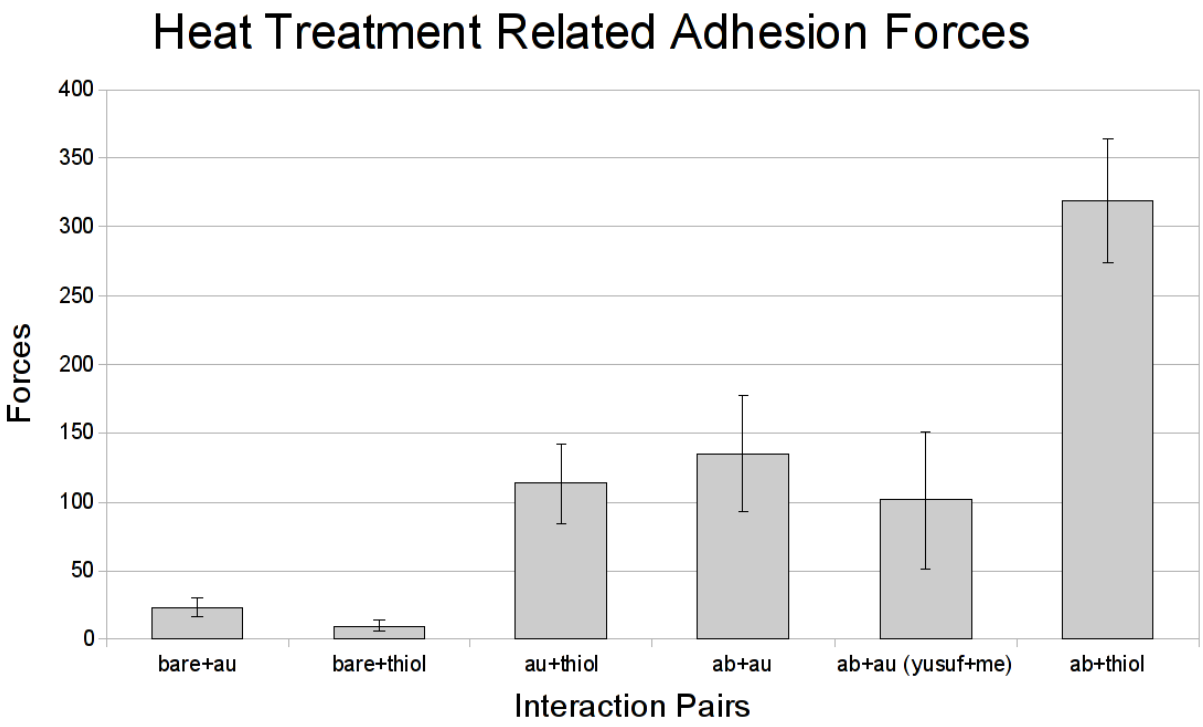

Fig 5.8 Adhesion forces of gold and other molecular recognition units for heat treatment related © K. Hao 2010

Stage	Five-Year Survival Rate (%)			
	Breast	Ovarian	Stomach	Lung
I(A)	100	93	78	47
II(A)	92	79	58	26
III(A)	67	51	20	8
IV(A)	20	17.5	8	2

Table 5.1 Average five-year survival rates form stage of first diagnosis for different cancer types.

Coating on Tip	Substrate
Taxol	Gold
LHRH	Gold
Antibody	Gold
Antibody	Taxol
LHRH	Taxol

Table 5.2 Substrates and coated tip materials used in the AFM study © Y. Oni 2010

APPENDIX A

In the course of preparing a gold chloride solution for the biosynthesis process, a stainless steel spatula was used to take some of the gold salt into solution. Initially it was observed that some black substance was formed on the stainless steel spatula when it came into contact with the gold salt. In order to know more on what was the cause for the black substance, a new stainless steel spatula was left in a gold chloride solution of concentrations of 1mM and10mM for 48 hours.

It was observed at the end of the 48 hour period that, the yellow gold chloride solution turned purple and dark purple respectively for the two solutions.

APPENDIX B

ΔT	Steady state temperature
I	Laser power
η	transduction efficiency
m_i	mass of the components of the system
$Cp,_I$	Heat capacity of the components of the system
Q_I	Rate of energy supplied to the system
Qext	Rate of energy flowing out of the system
A_λ	Absorbance of nanoparticle solution
Iopt	Optical path
c	Molar concentration
ε	Extinction coefficient
h	Heat transfer coefficient
s	Cross sectional area perpendicular to conduction
T*	Temperature difference
A	Rate of energy absorption
B	Rate constant associated with heat loss

5.4 References

[1] S. He et al, Materials Letters 61(2007) 3984-3987.

[2] Y.O. Oni, Implantable biomedical device and nanoparticles for cancer treatment.p155-171

[3] M.P. Melancon, W. Lu, C. Li, MRS Bulletin 34: 415-421, 2009.

[4] K. Hao, Gold nanoparticles in Cancer treatment a comparison of Adhesion forces

[5] A. Nakajima, World J. Microbiol. Biotechnol., 2003, 19, 369

[6] M.Gericke, A. Pinches, Microbial Production of Gold nanoparticles